Check for updates

FIBROSIS

Spatial genomics: Mapping the landscape of fibrosis

Prasad Palani Velu[1]†, Roxanna E. Abhari[1]†, Neil C. Henderson[1,2]*

Copyright © 2025 The Authors, some rights reserved; exclusive licensee American Association for the Advancement of Science. No claim to original U.S. Government Works

Organ fibrosis causes major morbidity and mortality worldwide. Treatments for fibrosis are limited, with organ transplantation being the only cure. Here, we review how various state-of-the-art spatial genomics approaches are being deployed to interrogate fibrosis across multiple organs, providing exciting insights into fibrotic disease pathogenesis. These include the detailed topographical annotation of pathogenic cell populations and states, detection of transcriptomic perturbations in morphologically normal tissue, characterization of fibrotic and homeostatic niches and their cellular constituents, and in situ interrogation of ligand-receptor interactions within these microenvironments. Together, these powerful readouts enable detailed analysis of fibrosis evolution across time and space.

INTRODUCTION

Fibrosis is not a disease but rather the outcome of tissue repair that has become dysregulated after various types of iterative tissue injury, notably chronic inflammation. Acute tissue injury elicits dynamic changes that facilitate tissue repair and restitution. However, in the face of overwhelming or persistent injury, the tissue microenvironment is markedly altered, resulting in the deposition of extracellular matrix (ECM) components that disrupt normal tissue architecture and function, ultimately leading to organ failure (*1*–*4*). It is estimated that 45% of deaths in the industrialized world are due to organ fibrosis (*1*, *2*, *4*), and there are very few antifibrotics are approved for use in clinical practice (*5*). It is, therefore, critical that we understand the cellular and molecular mechanisms regulating the initiation, persistence, and regression of fibrosis to facilitate the development of effective antifibrotic therapies.

Single-cell genomics has revolutionized our understanding of tissue fibrosis by allowing the study of cell populations and their interactions in health and disease at unprecedented resolution. However, single-cell and single-nucleus RNA sequencing (scRNA-seq and snRNA-seq, respectively) workflows involve tissue dissociation with resultant loss of spatial information. Spatial genomics approaches preserve spatial context and the relationships of cells within intact tissue, yielding valuable insights into fibrotic niche organization and how this links to biological function (*6*). Here, we provide an overview of cutting-edge spatial genomics approaches and how these technologies are increasing our understanding of fibrosis pathogenesis across organ systems. We then discuss the integration of spatial genomics information with other multimodal datasets and how these approaches are being leveraged to enhance both diagnostics and therapeutics in the field of organ fibrosis.

SINGLE-CELL GENOMICS IN ORGAN FIBROSIS

Single-cell genomics approaches have already transformed our understanding of the pathobiology of fibrosis (*7*–*12*). Single-cell experimental workflows commonly involve several steps: tissue processing to obtain a single-cell suspension, followed by single-cell capture, reverse transcription, amplification of cDNA, library construction, sequencing, and, lastly, computational analysis (*12*, *13*). Data from these experiments can be used to computationally group cells on the basis of their gene expression profiles, infer ligand-receptor interactions between populations of cells, and impute cellular differentiation trajectories by ordering cells in pseudotime (*14*).

Commonly used single-cell genomics approaches can be divided into scRNA-seq, where mRNA from the entire cell is captured and sequenced, and snRNA-seq, where mRNA is obtained from individual nuclei (excluding cytoplasmic mRNA transcripts) (*7*, *15*). There are relative advantages and disadvantages to both approaches, with the research question, tissue type, and cell type of interest being key determinants when selecting a modality (*13*, *16*). Advantages of snRNA-seq are reduced dissociation bias and reduced dissociation-induced transcriptional stress responses (*17*). Additionally, snRNA-seq can be performed on frozen samples, allowing researchers to pool samples obtained at different time points for processing, including those that have been stored in biobanks, greatly facilitating the generation of larger "*n*" datasets from rare conditions collated via multicenter collaborative networks (*18*). There are context-specific limitations with the sensitivity of snRNA-seq, however, such as ambient RNA complicating the annotation of less-abundant cell types or the reduced detection of microglial activation genes compared with that of scRNA-seq (*19*, *20*). Where possible, combinatorial approaches may be favored to maximize transcriptomic insights from the cell lineages of interest (*21*).

The generation of a single-cell or single-nucleus suspension involves a combination of tissue dissection, mechanical dissociation, and enzymatic digestion (*22*). These steps can potentially bias the cell populations isolated from tissue and induce stress-associated transcriptomic changes, although this is less of a concern when isolating nuclei (*18*, *23*, *24*). Tissue preparation can be particularly challenging when studying fibrotic tissue because cells may be enmeshed deep within the ECM, reducing their accessibility and necessitating harsher digestion protocols to liberate them (*22*). The use of dissociated cells or nuclei in conventional single-cell genomics approaches crucially results in the loss of spatial information. Downstream validation and spatial annotation of cellular subpopulations and therapeutic targets of interest identified using single-cell genomics methodologies is critical and can be performed using protein immunostaining or in situ hybridization (ISH) (*25*). Although these approaches can provide insights into the spatial organization of the cells and targets under investigation, they are often technically challenging (requiring the

[1]Centre for Inflammation Research, Institute for Regeneration and Repair, Edinburgh BioQuarter, University of Edinburgh, Edinburgh EH16 4UU, UK. [2]MRC Human Genetics Unit, Institute of Genetics and Cancer, University of Edinburgh, Edinburgh EH4 1QY, UK.
*Corresponding author. Email: neil.henderson@ed.ac.uk
†These authors contributed equally to this work.

Downloaded from https://www.science.org at Shanghai Jiao Tong University on June 30, 2025

optimization of antibodies), time consuming, and undertaken in a supervised manner, limited by the number of dyes that can be multiplexed in a given immunostaining system (Fig. 1) (*26*).

In the context of fibrosis research, single-cell genomics approaches have been used to comprehensively survey cell types and cell states in healthy and fibrotic tissues in different organs (*8*, *27*–*31*). Key findings from these studies have included the identification of distinct subpopulations of immune, mesenchymal, endothelial, and epithelial cells that are enriched in end-stage organ fibrosis compared with those in healthy tissue. In the fibrotic liver, specific groups of monocyte-derived macrophages, T cells, and mesenchymal cell subpopulations have been identified (*8*, *32*–*36*). In the lung and heart, cell atlas studies have revealed heterogeneity and specialization across cell types in patients with end-stage idiopathic pulmonary fibrosis (IPF) (*27*, *30*, *31*, *37*, *38*) and after myocardial infarction (MI) (*28*, *39*, *40*). In the kidney and musculoskeletal system, distinct expanding macrophage populations in end-stage chronic kidney disease (CKD) (*9*) and dystrophic diseases (*41*) have been described. These studies have also revealed that cell-type identities across lineages are plastic and are likely influenced by the local tissue microenvironment (*42*). Therefore, an understanding of how fibrosis-specific cell types and states are organized and interact within the fibrotic niche is critical in the development of potent antifibrotic therapies.

SPATIAL GENOMICS

Spatial genomics is an interdisciplinary field enabling the mapping of gene expression in tissue and offers distinct advantages over conventional dissociation–based single-cell technologies. Visualizing gene expression within its spatial context allows the interrogation of organs at different scales: from a "zoomed-in" view of key cell-cell interactions to a "zoomed-out" view of tissue organization, as seen in the concepts of liver zonation, spatial heterogeneity of lung fibrosis, or asynchronous remodeling in Duchenne muscular dystrophy (DMD).

Spatial genomics approaches aid the development of spatially resolved reference maps, or cell atlases, of the types and organization of cells in health and at different stages of disease (*10*, *43*). These atlases can be used to answer questions pertaining to key events in the development of organ fibrosis, such as how the fibrotic niche evolves during disease progression and whether elements of this are conserved across organs. Beyond a cellular characterization of the fibrotic niche, spatial genomics enables mapping of ligand-receptor interactions within the tissue microenvironment, rather than having to infer them using data derived from dissociation-based methods (*14*).

A detailed evaluation of the spatial genomics technologies now in use is provided by these comprehensive reviews (*25*, *44*–*46*), and Table 1 summarizes the relative strengths and weaknesses of these methodologies. Briefly, spatial genomics can be categorized into two broad approaches: sequencing-based and imaging-based technologies (Fig. 2) (*14*). In sequencing-based techniques [such as GeoMx digital spatial profiling (DSP; NanoString), Stereo-seq, spatial transcriptomics (Visium) (*47*, *48*)], nucleic acids are extracted, amplified, and sequenced from spatially resolved locations within tissues, and positional information is encoded onto transcripts before next-generation sequencing (*46*). Tissues are typically sectioned onto unique slides that have a spatially barcoded array applied or indexed before library preparation. Each read—an RNA sequence captured, amplified, and sequenced—has a unique spatial barcode, which is used to map its spatial position, whereas the rest of the sequencing read is mapped to the genome to identify the transcript of origin,

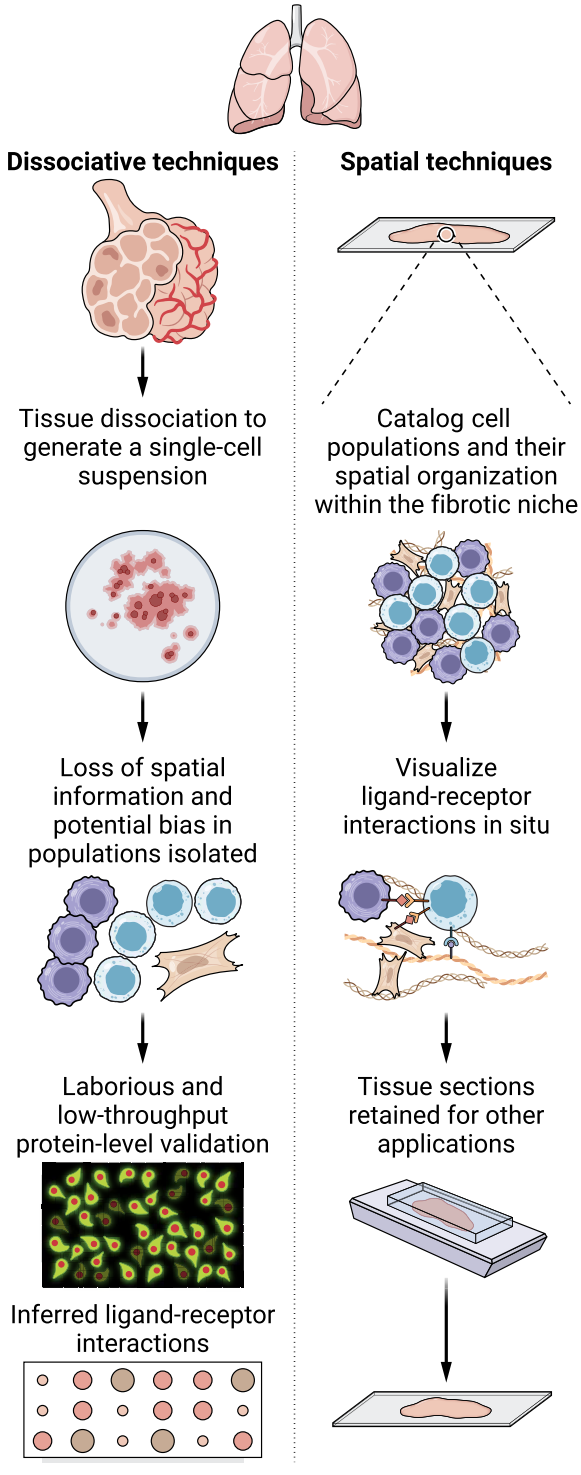
Dissociative techniques
Spatial techniques
Tissue dissociation to generate a single-cell suspension
Catalog cell populations and their spatial organization within the fibrotic niche
Loss of spatial information and potential bias in populations isolated
Visualize ligand-receptor interactions in situ
Laborious and low-throughput protein-level validation
Tissue sections retained for other applications
Inferred ligand-receptor interactions

Fig. 1. Comparison of dissociation-based single-cell transcriptomics and spatial genomics approaches. The use of dissociated cells or nuclei in conventional single-cell genomics approaches crucially results in the loss of spatial information, which is maintained in spatial genomics methodologies.

CREDIT: A. FISHER/SCIENCE TRANSLATIONAL MEDICINE

Downloaded from https://www.science.org at Shanghai Jiao Tong University on June 30, 2025

Table 1. A comparison of commonly used spatial genomics technologies. DBiT, deterministic barcoding in tissue; HDST, high-definition spatial transcriptomics.

Technology	Description and strengths	Limitations	Tissue type	Spatial resolution
		Imaging		
seqFish (*49*)	FISH-based approach using sequencing barcoding to detect multiple genes in singles cells; high multiplexing (hundreds of genes) due to combinatorial barcoding and multiple rounds of hybridization	Limited to predefined gene set; high computational demand	Fresh frozen	Single cell
MERFISH (*51*)	FISH-based approach using combinatorial barcoding and error correction ensuring high accuracy in gene detection despite photobleaching or incomplete hybridization	Limited to predefined gene set; requires extensive probe design and validation; high computational demand	Fresh frozen	Single cell
seqFISH^{+} (*161*)	Enhanced version of seqFISH; increased multiplexing capability (10,000+ genes), optimized probe sets, error robust barcoding, and fewer rounds of hybridization	Limited to predefined gene set; high computational demand; higher cost and increased protocol complexity	Fresh frozen	Single cell
CosMx (NanoString)	Multimodal profiling: resolves RNA and protein expression at single-molecule, subcellular resolution in situ; nucleus and membrane staining	High computational demand and cost; predefined panels	Fresh frozen, FFPE	Subcellular
Xenium (10x Genomics)	RNA location determination at subcellular resolution and can map cellular states; low false discovery rate; compatible with other 10x assays allowing multimodal analysis	Highly specific probes required; technical complexity and high computational demand	Fresh frozen, FFPE	Subcellular
ISS (*50*)	RNA sequenced directly within tissue sections by ligation (ISS and STARmap) or sequencing by synthesis (BaristaSeq)	Lower throughput compared with other methods	Fresh frozen, FFPE	Single cell
		Sequencing		
Visium manual + CytAssist (10x Genomics) (*47*)	Whole transcriptome analysis; manual placement on VISIUM slide or semi-automated with CytAssist	Fewer uniquely detected genes than with Visium CytAssist; lack of single-cell resolution	Fresh frozen, FFPE	55 μm
	Manual: one probe pair per coding gene. More flexibility and control over experimental conditions.			
	CytAssist: allows for analysis of samples with more degraded RNA (uses three probe pairs per coding gene)			
Visium HD (10x Genomics)	Slides contain two 6.5 mm–by–6.5 mm capture areas with continuous lawn of 2 μm–by–2 μm squares, achieving near single-cell spatial resolution.	High sequencing cost due to low resolution	Fresh frozen, FFPE	2 μm

(*Continued*)

Downloaded from https://www.science.org at Shanghai Jiao Tong University on June 30, 2025

(*Continued*)

Technology	Description and strengths	Limitations	Tissue type	Spatial resolution
Slide-seqV2 (*162*)	Slide-based system with random spatial bead spreading and in situ seq decoding	Bead density limits spatial resolution	Fresh frozen	10 μm
Seq-scope (*163*)	Illumina or MGI seq for oligo patterning on flow cells; barcode calling directly performed on the sequencer	High sequencing cost due to low resolution	Fresh frozen	<1 μm
Stereo-seq (*48*)	Illumina or MGI seq for oligo patterning on flow cells; barcode calling directly performed on the sequencer	High sequencing cost due to high resolution	Fresh frozen	0.22 μm
HDST (*120*)	Ultradense spatially barcoded beads resulting in very fine spatial resolution in subcellular detail	High sequencing cost due to high resolution	Fresh frozen	2 μm
DBiT-seq (*164*)	Uses microfluidic platform to apply barcoded oligos directly delivered to tissue in a grid-like spatial distribution; can profile protein and RNA in the same tissue	Microfluidic device required; lack of single-cell resolution	Fresh frozen	10 μm
XYZeq (*165*)	3D mapping of RNA expression; tissue placed on spatially barcoded microwell array for reverse transcription; then, whole cells are removed and undergo single-cell sequencing	Limitations to number of cells captured	Fresh frozen	500 μm
sci-Space (*166*)	Tissue placed on slide with spatially gridded oligos; nuclei then extracted, fixed, and sequenced; combinatorial barcoding without the need for predefined barcoded spots	Limitations to number of nuclei captured; lower transcript capture	Fresh frozen	118.2 to ~174.6 μm
Curio Trekker (*132*)	Converts single cell to spatial data; barcode released into the cells on a tissue slide, which are then processed for single-nucleus sequencing	High sequencing cost due to low resolution	Fresh frozen	<10 μm
GeoMx DSP (NanoString)	Photo-cleavable oligo tags attached to antibodies or hybridization probes; multiomic profiling; integrates with histology staining as nondestructive	Substantial process run time; limited resolution	Fresh frozen, FFPE	5 μm

Downloaded from https://www.science.org at Shanghai Jiao Tong University on June 30, 2025

together generating a gene expression matrix. These sequencing or capture-based techniques provide high-throughput and genome-wide information, with recent advancements enabling single-cell spatial resolution (for example, Visium HD).

Imaging-based approaches comprise in situ sequencing (ISS) and ISH methods, where fluorescently labeled probes targeting specific nucleic acids or antibodies targeting proteins are applied to tissue sections. The probes are then imaged by fluorescence microscopy and associated with a cell nucleus using image analysis methods to interrogate spatial gene expression. Imaging-based approaches [sequential fluorescence in situ hybridization (seqFISH), spatially resolved transcript amplicon readout mapping (STARmap), barcode in situ targeted sequencing (BaristaSeq), multiplexed error-robust fluorescence in situ hybridization (MERFISH), CosMx (NanoString), and Xenium (10x Genomics) (*49*–*51*)] offer single-cell spatial resolution and direct visualization but have lower throughput, and the breadth of transcripts that can be assayed is limited.

Inherent within many spatial genomics methods is concurrent histological evaluation with hematoxylin and eosin or fibrosis-specific stains such as picrosirius red, Masson's trichrome, or Movat's

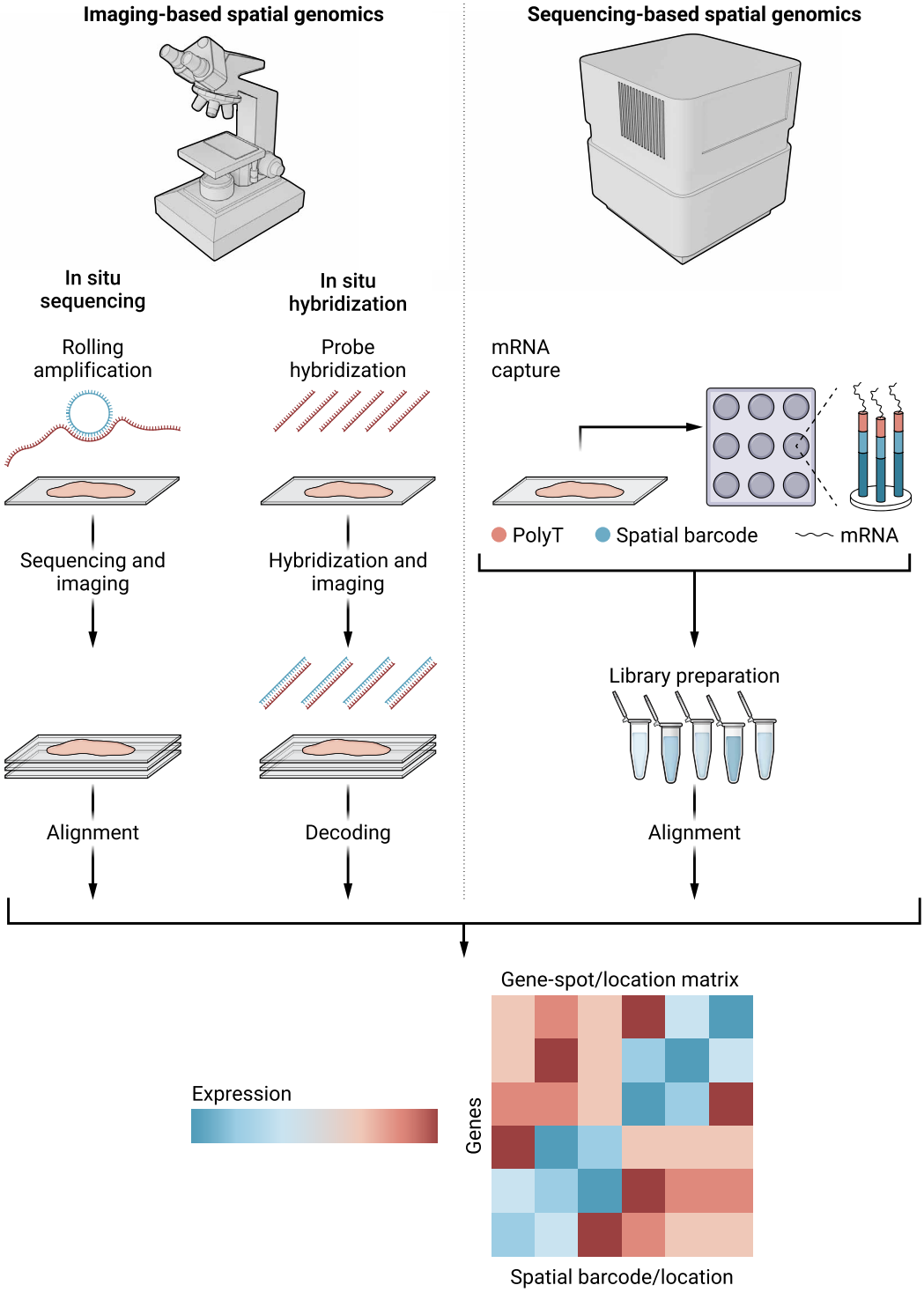

Fig. 2. Overview of imaging-based and sequencing-based spatial genomics approaches. Both approaches result in the formation of a gene or spot to location matrix, facilitating the preservation of spatial information in the downstream analysis of spatial genomics data.

pentachrome stains, which enable the identification of regions of interest and the precise geolocation of transcriptomic changes. Spatial genomics approaches are commonly performed in combination with high-resolution dissociation-based scRNA-seq or snRNA-seq approaches to generate high-resolution reference datasets. These datasets are then used in combination with spatial genomics to facilitate the deconvolution of regions of interest and provide information on the fraction of localized cell types. This approach is most often used to overcome the lack of single-cell resolution afforded by many current commercially available sequencing-based spatial

CREDIT: A. FISHER/SCIENCE TRANSLATIONAL MEDICINE

Downloaded from https://www.science.org at Shanghai Jiao Tong University on June 30, 2025

genomics approaches. This combinatorial analysis can be performed using publicly available reference datasets but is often performed on remaining tissue from the same sample that has not been used for spatial genomics, increasing the richness of the dataset and strength of conclusions that can be drawn from these data.

The analytical approaches used to interrogate spatial genomics datasets are rapidly evolving (*25*, *52*, *53*). A consensus on the "optimal" pipeline for analyzing spatial genomics data understandably does not exist; steps and packages used in any analytical pipeline will depend heavily on the spatial genomics method used, the type of tissue assayed, and the research question posed.

Some of the approaches and packages that are now being used to analyze spatial genomics data are summarized in Fig. 3. Briefly, data from imaging and sequencing-based methodologies first need to be processed and normalized before downstream analysis. Initial processing of raw data requires method-specific pipelines that correlate reads to spatial information to generate a gene or cell by location matrix, followed by normalization. Normalized spatial genomics data can then largely undergo downstream analytical processes similar to those performed on disaggregated single-cell transcriptomic data, depending on the specific research question. Last, data are visualized to facilitate data interpretation and dissemination.

Processing imaging-based spatial genomics data requires initial image registration or "horizontal integration" of imaging data: filtering out background noise, realigning scanned images after multiple rounds of hybridization, and stitching together different fields of view (*25*, *54*). Image registration is often technique-specific (MERFISH, NanoString CosMx, and 10x Genomics Xenium); however, general purpose pipelines such as Starfish are emerging (*55*). Because many imaging-based methods facilitate data capture at a subcellular resolution, detected transcripts need to be assigned to individual cells by a processed termed segmentation, effectively transforming a gene-spot matrix to a gene-cell matrix. This is a challenging but essential step given that many downstream analytical pipelines are optimized for use on single cells. Accurate cell segmentation is more challenging when analyzing fibrotic tissue because cellular density, morphology, and overall tissue architecture can vary by region. General approaches to segmentation include nucleus-based segmentation, cell membrane–based segmentation, and deep learning–based or transcript density–based approaches facilitated by packages including Proseg, Baysor, BIDCell, and RedeFISH (*56*–*59*).

Preprocessing of sequencing-based spatial genomics data involves alignment of raw captured mRNA sequences to the genome, matching of read barcodes to spatial locations, and quantification of reads at each spatial location, resulting in a gene-spot matrix. For 10x Visium technology, this process is facilitated by their proprietary Space Ranger software.

Normalization is an essential step to minimize technical variation by accounting for differences in mRNA capture

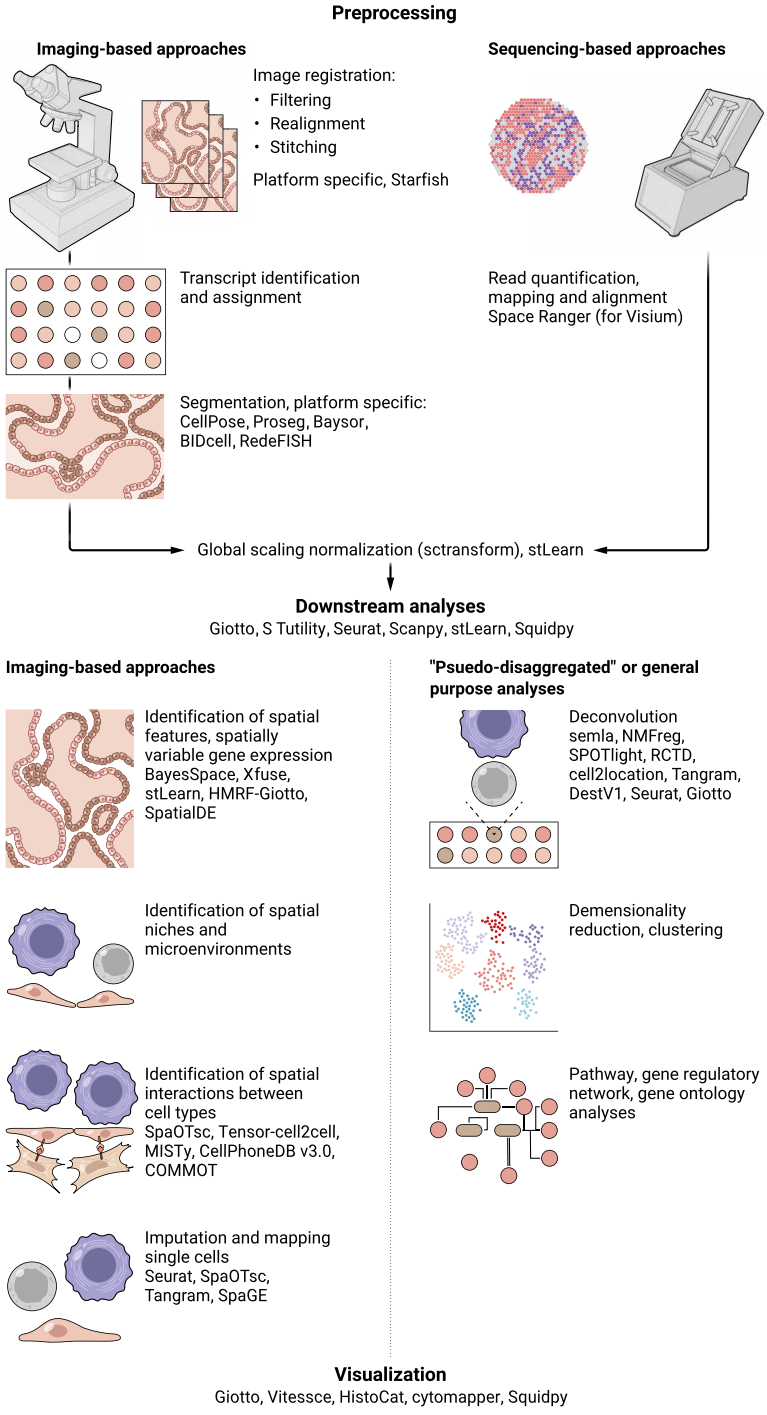
Preprocessing
Imaging-based approaches
Image registration:
• Filtering
• Realignment
• Stitching
Platform specific, Starfish
Sequencing-based approaches
Transcript identification and assignment
Read quantification, mapping and alignment Space Ranger (for Visium)
Segmentation, platform specific: CellPose, Proseg, Baysor, BIDcell, RedeFISH
Global scaling normalization (sctransform), stLearn
Downstream analyses
Giotto, S Tutility, Seurat, Scanpy, stLearn, Squidpy
Imaging-based approaches
Identification of spatial features, spatially variable gene expression BayesSpace, Xfuse, stLearn, HMRF-Giotto, SpatialDE
Identification of spatial niches and microenvironments
Identification of spatial interactions between cell types SpaOTsc, Tensor-cell2cell, MISTy, CellPhoneDB v3.0, COMMOT
Imputation and mapping single cells Seurat, SpaOTsc, Tangram, SpaGE
"Psuedo-disaggregated" or general purpose analyses
Deconvolution semla, NMFreg, SPOTlight, RCTD, cell2location, Tangram, DestV1, Seurat, Giotto
Demensionality reduction, clustering
Pathway, gene regulatory network, gene ontology analyses
Visualization
Giotto, Vitessce, HistoCat, cytomapper, Squidpy

Fig. 3. Summary of spatial genomic data analysis pipeline. Initial processing of raw data requires method-specific pipelines that correlate reads to spatial information to generate a gene or cell by location matrix, followed by normalization. Normalized spatial genomics data can then largely undergo downstream analytical processes similar to those performed on disaggregated single-cell transcriptomic data, depending on the specific research question. Last, data are visualized to facilitate data interpretation and dissemination. HMRF, hidden Markov random field; RCTD, robust cell-type decomposition. References for listed packages: Starfish (*55*), CellPose (*56*), Proseg, Baysor (*57*), BIDCell (*58*), RedeFISH (*59*), BayesSpace (*139*), Xfuse (*140*), stLearn (*141*), Giotto (*61*), SpatialDE (*142*), semla (*143*), NMFreg (*144*), SPOTlight (*145*), RCTD (*146*), cell2location (*147*), Tangram (*148*), DestVI (*149*), Seurat (*150*), SpaOTsc (*151*), Tensor-cell2cell (*152*), MISTy (*153*), CellPhoneDB 3.0 (*154*), COMMOT (*155*), SpaGE (*156*), Vitessce (*157*), HistoCat (*158*), cytomapper (*159*), and Squidpy (*160*).

CREDIT: A. FISHER/SCIENCE TRANSLATIONAL MEDICINE

Downloaded from https://www.science.org at Shanghai Jiao Tong University on June 30, 2025

across tissue, which is particularly important in sequencing-based approaches where the mRNA capture rate can be lower (*25*). Several normalization approaches can be used with spatial genomics data, including dividing each cell in a gene-spot matrix by the total number of spots (Scanpy and Giotto). Normalizing per group of genes so that all genes have similar abundances (sctransform) can be preferable for tissues where cell densities (and, thus, mRNA abundances) vary across the tissue section (*52*, *60*–*63*). Downstream analysis of normalized, spatially orientated data can be broadly categorized into spatially focused applications (spatially differential gene expression, identification of spatial niches or microenvironments, and determination of spatial interactions between cells and cell-type imputation) or general purpose "pseudo-disaggregated" approaches resembling conventional single-cell transcriptomics analysis (deconvolution, dimensionality reduction, clustering, differential gene expression, and pathway analysis).

INVESTIGATING FIBROSIS USING SPATIAL GENOMICS

Spatial genomics approaches have rapidly evolved in the past few years and have been harnessed to study fibrosis in several organ systems (Table 2) (*64*). Below, we discuss some key examples.

Liver

Spatial genomics methods have been used to expand on the findings made using dissociation-based single-cell approaches in studying the liver in homeostasis and fibrosis (*7*, *8*, *42*). Chung *et al.* used a sequencing-based approach (Visium, 10x Genomics) to characterize the cellular landscape across multiple chronic liver disease etiologies, including primary sclerosing cholangitis (PSC), primary biliary cholangitis (PBC), and alcohol-related liver disease (ALD) (*65*). They demonstrated excellent correlation between histological annotation (normal versus fibrotic) and detectable alterations in gene expression signatures. Cell-type deconvolution performed using reference scRNA-seq data localized higher proportions of pathogenic mesenchymal cells (*ACTA2*$^+$, *FABP4*$^+$, and *COL3A1*$^+$), tissue monocytes (*IL17RA*$^+$ *S100A8*$^+$ and *FCER1G*$^+$), Kupffer cells (*VCAM1*$^+$ and *SDC3*$^+$), T cells (*CCL4*$^+$ *CCL5*$^+$ *KLRB1*$^+$ and *GZMA*$^+$ *IL17RA*$^+$) and B cells (*HLA-DR*$^+$, *CD37*$^+$ *CXCR4*$^+$, and *IGHM*$^+$ *IGHG*$^+$) to fibrotic areas in cirrhotic explants (*65*). In fibrotic regions across all etiologies, there was an enrichment of hepatic stellate cells (*ACTA2*$^+$ and *FABP4*$^+$) and scar-associated mesenchymal cells (*COL3A1*$^+$). This unbiased spatial transcriptomics approach allowed corroboration of key findings from previous scRNA-seq–based liver fibrosis studies, not only confirming the presence of previously described disease-specific cell populations but also determining their spatial location in fibrotic or normal parenchyma, indicating their potential function and denoting hubs of intercellular communication.

In investigating human healthy, PSC, and PBC liver tissue using a combination of spatial genomics methods [Visium (10x Genomics) and GeoMx DSP (NanoString)], analysis of consecutive *z*-stack slices demonstrated diversity within the macrophage compartment (*66*). These spatial data corroborated findings generated using scRNA-seq and snRNA-seq, with particular relevance to liver zonation, identifying the spatial organization of natural killer, T, and B cell populations in the periportal region; MHCII$^+$ (major histocompatibility complex class II), lipid-associated macrophages, and Kupffer cells in the pericentral region; and activated macrophages localized to the periportal area. Co-localization of *CD4*$^+$ T cells, *CCL19*$^+$ stellate cells, and *CCL21*$^+$ liver sinusoidal endothelial cells was observed, identifying a node of immune-mesenchymal-endothelial signaling within the fibrotic niche (*66*). This study also defined the enrichment of transitioning cholangiocyte-like hepatocytes devoid of their zonated signature located in "border" regions around the perimeter of scars in PSC liver tissue. Scar-associated *TREM2*$^+$ and monocyte-like macrophages (with up-regulated expression of *LGALS3*, *SPP1*, and *ADA2*) were observed around cholangiocytes in the center of fibrotic regions with concentric periductular fibrosis, whereas Kupffer cells were localized outwith scar regions, indicating topographically differential immune signaling (*8*, *66*, *67*).

Using imaging-based spatial genomics (MERFISH), Watson *et al.* delineated three zonally restricted hepatocyte populations in healthy liver and identified two disease-associated hepatocyte populations in fibrotic liver, which were distributed throughout the lobules, with no zonal restriction (*68*). These disease-associated hepatocyte populations were expanded in fibrosis (*68*). Interrogation of zonally enriched ligand-receptor interactions identified hepatic stellate cell (HSC) and macrophage thrombospondin (THBS1/2) signaling to CD36$^+$ hepatocytes in the pericentral region, which the authors postulated could be involved in the pathogenesis of metabolic dysfunction–associated steatotic liver disease (*68*, *69*).

Lung

Lung fibrosis is characterized by dense fibroblast accumulation in whorl-like structures (called fibroblastic foci), with adjacent hyperplastic alveolar epithelial cells and distortion of airway architecture (*70*, *71*). Spatial and temporal heterogeneity in the distribution of fibrotic foci is a hallmark histological finding in pulmonary fibrosis. These factors make spatial genomics–based analyses of pulmonary fibrosis an exciting area.

Spatial genomics analyses across large tissue areas in human IPF have enabled the detection of transcriptionally altered cell states and populations in morphologically normal areas, even when compared with similarly annotated areas from controls (*72*–*74*). Along a gradient from normal tissue toward fibrotic foci (morphologically normal → transition zones containing fibroblastic foci → areas of dense honeycombing with honeycomb epithelial metaplasia), there was a demonstrable increase in collagen gene expression, along with the emergence of pathological epithelial cell populations, increased numbers of myofibroblasts, and reduced numbers of endothelial cells (*72*). Along a similarly annotated gradient in IPF, Blumhagen *et al.* described the loss of alveolar parenchymal markers, gain of secretory cell markers, dysregulation of activating transcription factor 4, and increased eukaryotic initiation factor (EIF2) signaling zones between morphologically normal alveolar tissue and areas of dense fibrosis (*73*). These unbiased assessments of the cellular transcriptome along gradients of disease enable the identification of changes in earlier disease stages and pinpoint signaling pathways modulating disease progression, collectively facilitating the identification of the key therapeutic targets in early disease.

Sequencing-based spatial genomics analysis (GeoMx DSP, NanoString) of human IPF sections demonstrated co-localization of *KRT5*$^-$/*KRT17*$^+$ aberrant basaloid (AbBa) cells with myofibroblasts within the fibrotic niche preferentially located around airways, with these populations communicating via the Ephrin signaling pathway and demonstrating an increased senescence gene score (*75*). This study also describes two corollary niches in disease: an airway

Downloaded from https://www.science.org at Shanghai Jiao Tong University on June 30, 2025

macrophage niche containing secreted phosphoprotein 1 (SPP1)$^+$ macrophages, adjacent to the fibrotic niche in the lumen of distal airways, and an immune niche comprising distinct lymphoid cell foci in fibrotic tissue, surrounded by remodeled bronchial vessels lined by plasmalemma vesicle associated protein (PLVAP)$^+$ endothelial cells. The authors subsequently validated these observations using an imaging-based spatial genomics approach (Xenium, 10x Genomics) and multiplexed COMET protein immunofluorescence (*75*). Using sequencing-based approaches (Visium, 10x Genomics), Franzén *et al.* similarly describe a fibrotic niche comprising AbBa epithelial cells co-localizing with myofibroblasts and nearby profibrotic macrophages, dominated by transforming growth

Table 2. Summary of spatial genomics studies in organ fibrosis. CTD-ILD, connective tissue disease–associated interstitial lung disease; cHP, chronic hypersensitivity pneumonitis; NSIP, nonspecific interstitial pneumonia; NFKBIZ, NF-kappa-B inhibitor zeta; TREM2, triggering receptor expressed on myeloid cells 2.

Authors (reference)	Human/mouse	Disease/model	Spatial genomics method	Key findings
		Liver		
Chung *et al.* (*65*)	Human	PSC, PBC, and ALD	Visium (10x Genomics)	Distinct transcriptomic signatures correspond with histological annotation.
				Altered proportions of pathogenic cell types in fibrotic areas
Andrews *et al.* (*66*)	Human	PSC and PBC	Visium (10x Genomics) and GeoMx DSP (NanoString)	Node of intercellular signaling within the fibrotic niche comprising CD4$^+$ T cells, CCL19$^+$ stellate cells, and CCL21$^+$ liver sinusoidal endothelial cells
				Enrichment of transitioning cholangiocyte-like hepatocytes around perimeter of PSC scars
				Localization of scar-associated TREM2$^+$ macrophages and monocytes around cholangiocytes in the center of fibrotic regions
Watson *et al.* (*68*)	Human	Liver fibrosis	MERFISH	Zonal enrichment of receptor-ligand interactions
				Two fibrosis-specific hepatocyte populations that expand with injury and are not zonally restricted; new bridging pattern of HSCs across the lobule
		Lung		
Eyres *et al.* (*72*)	Human	IPF	GeoMx DSP (NanoString)	Distinct transcriptomic signatures associated with areas of disease and in histologically unaffected areas
				Altered homeostatic and pathogenic cell populations within fibrotic niche
				Loss of alveolar epithelial NFKBIZ expression and resultant IL-6 axis disruption
Blumhagen *et al.* (*73*)	Human	IPF	GeoMx DSP (NanoString)	Transcriptomic alterations in histologically normal-appearing areas in IPF tissue
				Activation of ER stress and deactivation of wound-healing pathways in areas of dense fibrosis
				Increased EIF2 signaling in IPF lung

(*Continued*)

Downloaded from https://www.science.org at Shanghai Jiao Tong University on June 30, 2025

(*Continued*)

Authors (reference)	Human/mouse	Disease/model	Spatial genomics method	Key findings
Vannan *et al.* (*74*)	Human	IPF, CTD-ILD, cHP, NSIP, and sarcoidosis	Xenium (10x Genomics)	Identification of regions where *KRT5*$^{-}$/*KRT17*$^{+}$ cells appear to have detached from underlying basement membranes
				Molecularly defined spatial niches
				Machine learning–derived model of disease pathogenesis in IPF
Mayr *et al.* (*75*)	Human	IPF	Visium (10x Genomics) and Xenium (10x Genomics)	Cellular and molecular composition of fibrotic (myofibroblasts and AbBa cells), airway macrophage (SPP1^{+} macrophages), and immune (lymphoid cells surrounded by remodeled endothelial vessels) niches
Franzén *et al.* (*76*)	Human and mouse	IPF and bleomycin	Visium (10x Genomics)	Role for APOE signaling in IPF pathogenesis
				Spatial interrogation of epithelial regenerative pathways
Kurche *et al.* (*80*)	Human	IPF	DSP (NanoString)	Reduced expression of small airway secretory cell markers (SFTPB and SCGB3A2) in morphologically normal *MUC5B* variant IPF specimens
		Heart		
Lacraz *et al.* (*82*)	Mouse	Ischemia reperfusion injury	Tomo-seq	SOX9 as a key transcription factor in cardiac fibrosis
Jung *et al.* (*83*)	Mouse	MI	Visium (10x Genomics)	Up-regulation of *Trem2* expression in macrophages during late phase post-MI
Ko *et al.* (*84*)	Mouse	MI	Visium (10x Genomics)	Novel fibrogenic pathway regulated by cardiac fibroblasts: Htra3-TGFβ-IGFBP7
Kuppe *et al.* (*28*)	Human	MI	Visium (10x Genomics)	Characterization of MI border zone niche: transition between injured and uninjured cells marked by graded *ANKRD1* and *NPPB* expression
				Distinct myofibroblast and activated phagocytic macrophages (*SPP1*$^{+}$*CD36*$^{+}$) interaction
Amrute *et al.* (*85*)	Human	MI	Visium (10x Genomics)	Niche-specific macrophage, T cell, and fibroblast interactions
				IL-1β–mediated CCR2^{+} macrophage and FAP^{+} fibroblast signaling
Kanemaru *et al.* (*10*)	Human	Uninjured (transplant donors)	Visium (10x Genomics)	Identification of ventricular-myocardial stress niche, intercellular interactions mediated by TGFβ superfamily
		Kidney		

(*Continued*)

Downloaded from https://www.science.org at Shanghai Jiao Tong University on June 30, 2025

(*Continued*)

Authors (reference)	Human/mouse	Disease/model	Spatial genomics method	Key findings
Dixon *et al.* (*90*)	Mouse (females)	Ischemia-reperfusion injury	Visium (10x Genomics)	T cell and macrophage interactions with proximal tubule cells in an injured state denoting an AKI-to-CKD transition
Polonsky *et al.* (*91*)	Mouse	Ischemia-reperfusion injury	seqFISH	Distinct AKI-associated niche comprising *Vcam1*$^+$ proximal tubule epithelial cells (ECs), fibroblasts and immune cells; *Clcf1-Crlf1* signaling between injured ECs and fibroblasts
Clair *et al.* (*99*)	Human	AS, FSGS, and MN	GeoMx DSP (NanoString)	Transcriptional differences are histologically similar glomeruli.
				Up-regulation in *GJA5*, *TNS1*, and *CCND1* common to all biopsies indicating potential utility as biomarkers
Lake *et al.* (*96*)	Human	AKI and CKD	SLIDE-seq2, Visium (10x Genomics)	Abnormal epithelial cells (proximal tubule and tall ascending limb loop of Henle) co-localize with distinct inflammatory immune cells and fibrotic stromal cells, indicative of progression to CKD
Chen *et al.* (*97*)	Human	DKD	Visium (10x Genomics)	Increased inflammatory signaling (chemokines) in parenchymal cells
				Venous endothelial cells and CCL19$^+$ fibroblasts enriched in areas of renal fibrosis
Canela *et al.* (*98*)	Human	Renal calcium oxalate stone disease	Visium (10x Genomics)	Up-regulation of injury pathways in histologically unaffected areas (separate from areas with mineral deposition)
				MMP7 and MMP9 as biomarker candidates
Abedini *et al.* (*95*)	Human	CKD (hypertension and DKD)	Visium (10x Genomics) and CosMx (NanoString)	Detailed multimodal characterization of four distinct microenvironments including disease-specific fibrotic microenvironment
				Identification of *VCAM1*$^+$ and *HAVCR1*$^+$ injured proximal tubule cell state
		Skeletal muscle		
Coulis *et al.* (*41*)	Mouse	D2-*mdx* mice	Visium (10x Genomics)	Areas of Galectin-3 expression denote active pathology with adjacent up-regulation of Pdgfrα stromal cells.
				Interactions between disease-specific myeloid and mesenchymal cells mediated by *Spp1*

(*Continued*)

Downloaded from https://www.science.org at Shanghai Jiao Tong University on June 30, 2025

(*Continued*)

Authors (reference)	Human/mouse	Disease/model	Spatial genomics method	Key findings
Heezen *et al.* (*104*)	Mouse	*mdx* and D2-*mdx* mice	Visium (10x Genomics)	Identification of up-regulated genes corresponding with histopathology: muscle regeneration, fibrosis, and calcification
Stec *et al.* (*103*)	Mouse	D2-*mdx* mice	Visium (10x Genomics)	Increased fibrotic and inflammatory gene expression profiles in morphologically undamaged areas
Larouche *et al.* (*106*)	Mouse	VML	Visium (10x Genomics)	Characterization of VML defects: co-localization of $Trem2^+$ scar-associated macrophages and mesenchymal-derived cells with myogenic cells located peripherally

factor–β (TGFβ), TP53, and apolipoprotein E (APOE) signaling (*76*, *77*).

Extending on these findings linking transcriptional disruption and histological changes, Vannan *et al.* used a machine learning approach to segment individual airspaces, describing the evolution of transcriptomic changes in areas which were more extensively remodeled (*74*). The authors subsequently proposed a conceptual model of disease pathogenesis in IPF, where initial disruption of the alveolar-capillary interface leads to regenerative-associated programming of the epithelium, followed by subepithelial fibroblast activation and subsequent myeloid cell recruitment or proliferation (*74*). Notably, Vannan *et al.* identified numerous regions where AbBa cells appear to have detached from their basement membrane, exposing underlying activated fibroblasts, which the authors suggest could permit the migration of fibroblasts into the airspace to deposit ECM (*74*).

The murine equivalent of the AbBa epithelial cell is the $Krt8^+$ alveolar differentiation indeterminate (ADI) cell, derived from type 2 alveolar epithelial (AT2 cells) (*78*). Using spatial trajectory analysis of both murine bleomycin-induced pulmonary fibrosis and human IPF, Franzén *et al.* describe a linear epithelial reparative trajectory (AT2 → ADI → AT1) in murine disease in contrast with a divergent trajectory in human IPF, resulting in the generation of both AbBa epithelial cells and AT1 cells (*76*). The successful transdifferentiation of ADI to AT1 cells is thought to be a key determinant in the spontaneous resolution of fibrosis in the murine bleomycin model (*78*). $SCGB3A2^+$ secretory cells are a possible alternative source for AbBa cells, suggested by the proximity of these cells to the AbBa-containing fibrotic niche in human IPF sections (*31*, *76*). Arrested alveolar regeneration resulting in the persistence of AbBa epithelial cells presents a key area for further investigation and potential therapeutic target in the management of IPF (*30*, *31*, *74*, *76*).

Kurche *et al.* deployed spatial genomics (GeoMx DSP, NanoString) in IPF and control sections genotyped for the *MUC5B* promoter variant, a dominant risk factor for the development of IPF (*79*, *80*). Expression of small airway secretory cell (SASC) markers *SCGB3A2* and *SFTPB* was reduced in normal distal airways of *MUC5B* variant carriers, suggesting a correlation between loss of SASCs and the risk of developing pulmonary fibrosis (*80*).

Heart

Single-cell and spatial genomics technologies have improved our understanding of the mechanisms underpinning homeostasis, remodeling, and fibrosis after cardiac injury (*10*, *40*). Early iterations of spatial genomics approaches in human MI and mouse models of MI identified SRY-box transcription factor 9 (SOX9) as a key regulator of cardiac remodeling and fibrosis (*81*, *82*). Sequencing-based spatial genomics (Visium, 10x Genomics) applied to a murine MI model demonstrated considerable spatiotemporal dynamics in macrophages, with a potential pro-reparative role assigned to $TREM2^{hi}$ macrophages that emerge in areas of infarct (*83*). Combined scRNA-seq and spatial genomics analyses (Visium, 10x Genomics) in a murine MI model identified HtrA serine peptidase 3 (Htra3) as a key regulator of cardiac fibroblast function in the context of cardiac pressure overload, delineating a Htra3-TGFβ–insulin-like growth factor-binding pathway 7 (IGFBP7) pathway, which could potentially be modulated in the management of cardiac fibrosis (*83*, *84*).

Kuppe *et al.* performed concurrent snRNA-seq, single-nucleus assay for transposase-accessible chromatin using sequencing (snATAC-seq), and spatial genomics analysis (Visium, 10x Genomics) of human MI using cryosections from histologically distinct areas (fibrotic, necrotic, or unaffected left ventricular myocardium) obtained at various time points after onset of clinical symptoms, generating a rich multi-omic map of human MI. The authors identified a distinct border zone niche surrounding the injured myocardium, with distinct delineation between injured and uninjured cell types, marked by a gradient of *ANKRD1* and *NPPB* expression indicative of ventricular cardiomyocyte stress. Fibroblast and myeloid populations within fibrotic areas were heterogeneous, with a distinct cellular dependency between myofibroblasts and $SPP1^+CD36^+$-activated phagocytic macrophages (*28*).

Spatial genomics analysis of human MI tissue has also been used to characterize the inflammatory-fibrotic axis in MI and chronic heart failure (*85*). The emergence of fibroblast activation protein

Downloaded from https://www.science.org at Shanghai Jiao Tong University on June 30, 2025

alpha (FAP)$^+$ and periostin (POSTN)$^+$ fibroblasts after acute MI and in chronic heart failure was determined using cellular indexing of transcriptomes and epitopes by sequencing (CITE-seq; a dissociation-based technique enabling contemporaneous cell surface protein profiling) (*86*). Subsequent spatial genomics analysis (Visium, 10x Genomics) revealed immune-fibroblast interactions driven by interleukin-1β (IL-1β) signaling from CCR2$^+$ macrophages to FAP$^+$ fibroblasts in fibrotic areas, which was further validated in a murine model of cardiac fibrosis (*85*).

A multi-omic approach using spatial genomics in combination with scRNA-seq, snRNA-seq, and snATAC-seq defined a ventricular-myocardial stress niche in normal human hearts (*10*). This niche comprised fibroblasts with high activation signature genes and collagen expression (*POSTN*, *TNC*, *COL1A1*, *COL3A1*, and *FN1*) and ventricular cardiomyocytes exhibiting a distinct cardiomyocyte stress signature (*NPPB*, *LMCD1*, *XIRP2*, *ACTA1*, and *PFKP*), which co-localized with vascular cells and immune cells. Spatial ligand-receptor interaction analysis identified TGFβ superfamily signaling as the key pathway mediating cell-cell communication within this niche. Further evidence of fibroblast-cardiomyocyte interactions within the cardiac fibrotic niche was provided in a study by Kanemaru *et al.* using small-molecule fluorescence in situ hybridization (smFISH), demonstrating that *COL1A1*$^+$ fibroblasts and *NPPB*$^+$ cardiomyocytes are enriched and co-localize in tissue sections from individuals with dilated cardiomyopathy compared with those from controls (*10*). These studies demonstrate the ability of spatial genomics approaches to identify niches that can act as sources of pro-fibrogenic cells in disease and facilitate the identification of targets and pathways involved in fibrogenesis (*10*).

Kidney

Renal tubular injury and tubulointerstial fibrosis work in concert to manifest clinically as CKD (*87*). Acute kidney injury (AKI) is reversible in many cases but is a risk factor for subsequent development of CKD. Kidney fibrosis is a key driver of CKD, culminating in end-stage renal failure (*88*, *89*). Spatial genomics analysis (Visium, 10x Genomics) of a murine model of AKI [renal ischemia-reperfusion injury (IRI)] identified a distinct injured proximal tubule cell state and characterized T cell–macrophage interactions with these injured proximal tubule cells at late time points after injury (*90*). Imaging-based spatial genomics analysis (seqFISH) in a murine IRI model by Polonsky *et al.* facilitated the description of several distinct cellular microenvironments or niches, including a pathogenic niche in AKI (*91*). This niche comprised *Vcam1*$^+$ proximal tubule epithelial cells (with elevated expression of injury-response genes), which co-localized with injury-associated fibroblasts, endothelial, and immune cells (*91*). Injury-associated fibroblasts and endothelial cells within this niche communicated via spatially distinct *Clcf1-Crlf1* signaling, with *Clcf1* known to encode a member of the IL-6 cytokine family (*91*, *92*). These findings support the hypothesis that ongoing subclinical inflammation is associated with the transition from AKI to CKD (*90*, *93*). The determination of this spatial relationship builds on prior work using snRNA-seq on dissociated tissue, where the physiologic context of macrophage and leukocyte recruitment to areas of injury was unclear (*90*, *91*, *94*).

Abedini *et al.* used complementary spatial genomics approaches (Visium, 10x Genomics and CosMx, NanoString) to define distinct cellular microenvironments in healthy, diabetic, and hypertensive diseased human kidneys, detailing the emergence of a disease-specific fibrotic niche and a concurrent immune niche located within the fibrotic niche. Central to the fibrotic niche is a distinct injured proximal tubule cell type (*VCAM1*$^+$ and *HAVCR1*$^+$), enriched within areas of fibrosis in CKD samples, and interacting with endothelial cells and stromal cells expressing chemotactic factors (*CXCL12*, *CCL19*, and *CCL21*) (*95*). Corroborating these findings, sequencing-based spatial genomics [SLIDE-Seq2, Visium (10x Genomics)] analyses of human healthy, AKI, and CKD samples demonstrated that immune and stromal cells co-localized more frequently with abnormal epithelial cells, with increased inflammation and fibrosis in disease states compared with controls (*96*). Epithelial cells with maladaptive repair signatures had elevated cytokine production; increased interactions with distinct inflammatory and fibrotic cell types; and signatures indicative of senescence, down-regulated repair, and progression to CKD, corollary to features identified in spatial genomics analyses of murine IRI (*91*, *96*). Increased inflammatory signaling was also observed in spatial genomics analysis of human samples of diabetic kidney disease (DKD), a leading cause of renal fibrosis and CKD globally. Venous endothelial cells co-localized with *CCL19*$^+$ fibroblasts and immune cells and were enriched in areas of fibrosis, lending weight to the hypothesis that persistent inflammatory signaling and immune cell recruitment is associated with progressive renal fibrosis and the development of CKD (*97*).

Observations corollary to those made in CKD were made in spatial analysis (Visium, 10x Genomics) of tissue sections from individuals with calcium oxalate renal stone disease (*98*). Canela *et al.* provided detailed annotation and spatial orientation of papillary cells, defining an undifferentiated epithelial cell type that localized to regions of injury or mineral deposition. Up-regulation of injury pathways across multiple cell types in the renal papilla was discernible, even in areas spatially removed from mineral deposition. The authors hypothesize that papillary injury and inflammation initiate a cascade of profibrotic signaling and matrix remodeling, leading to the development of CKD in chronic renal stone disease. Matrix metalloproteinase 7 (MMP7) and MMP9 were spatially differentially expressed, corresponding to stone disease and mineral deposition, respectively, and could act as putative biomarkers of active stone disease, even in the absence of detectable renal impairment (*98*).

Clair *et al.* applied GeoMx DSP (NanoString) to kidney biopsies to investigate intra-glomerular transcriptional heterogeneity within and between patients with Alport's syndrome (AS), focal segmental glomerulosclerosis (FSGS), and membranous nephropathy (MN) (*99*). This analysis identified not only transcriptional heterogeneity among histologically diseased glomeruli but also transcriptional alterations among histologically nondiseased glomeruli compared with healthy control tissue, demonstrating the increased sensitivity of unbiased spatial genomics approaches to detect early changes in disease evolution. Several genes were noted to be up- and down-regulated across all conditions, with three genes—*GJA5*, *TNS1*, and *CCND1*—noted to be up-regulated in a whole-genome sequencing database of patients with glomerulopathies leading to nephrotic syndrome [Nephrotic Syndrome Study Network (NEPTUNE)] (*100*).

Skeletal muscle

Skeletal muscle fibrosis occurs in the context of muscular dystrophies (the commonest of which is DMD), myopathies, and severe injury, resulting in functional impairment (*101*). The *mdx* (muscular dystrophy X-linked mouse) and D2-*mdx* transgenic mouse models are commonly used as preclinical models of DMD. D2-*mdx* mice

Downloaded from https://www.science.org at Shanghai Jiao Tong University on June 30, 2025

manifest with a more severe phenotype and recapitulate the asynchronous degeneration seen in human DMD biopsies (*102*). In a spatial genomics analysis (Visium, 10x Genomics) of D2-*mdx* mice, 55-μm Visium spots could be denoted as high or low in galectin-3, with elevated galectin-3 expression noted in areas of active pathology (*41*). Genes commonly associated with fibrosis, including *Fn1*, *Postn*, *Pdgf*, and *Tgf*β, were up-regulated in galectin-3–high spots. Analysis of spots adjacent to galectin-3–high areas demonstrated increased expression of Pdgfrα stromal cells, suggestive of a myeloid-mesenchymal interaction in areas of tissue fibrosis. Interactome analysis using CellChat identified interactions between myeloid and mesenchymal cells to be mediated by *Spp1*. These findings were corroborated in human samples from a range of myopathies, including DMD, and inclusion body myositis with galectin-3$^+$ macrophages found to be in close apposition to platelet-derived growth factor receptor α$^+$ stromal cells (*41*).

A similar analysis in D2-*mdx* mice using Visium (10x Genomics) performed by Stec *et al.* identified heightened fibrotic and inflammatory gene expression profiles in morphologically undamaged regions interspersed between dystrophic regions (*103*). Regions surrounding early damage had an inflammatory gene expression profile, whereas those surrounding regions of intermediate regeneration demonstrated increased collagen deposition and fibroadipogenic progenitors. This observation lends weight to the hypothesis that inflammatory and regenerative signals can "propagate" to adjoining areas, driving inflammation and fibrosis (*103*).

Histopathological changes in the skeletal muscles of D2-*mdx* mice comprise areas of muscle regeneration, fibrosis, and calcification. These changes often overlap, making the identification of pathology-specific markers challenging. Heezen *et al.* used unbiased spatial context provided by a sequencing-based approach (Visium, 10x Genomics) in the D2-*mdx* mouse model to identify the up-regulation of specific genes in muscle regeneration (*Myl4*, *Sparc*, and *Hspg2*), fibrosis (*Vim*, *Fn1*, and *Thbs4*), and calcification (*Bgn*, *Ctsk*, and *Spp1*), before validating these findings using smFISH (*104*).

Skeletal muscle fibrosis also occurs in volumetric muscle loss (VML), where the acute loss of skeletal muscle due to trauma or surgery induces exuberant scar formation and fibrotic supplantation, leading to loss of function (*105*). Spatial genomics analyses (Visium, 10x Genomics) in a murine experimental model of VML demonstrated the co-localization of Trem2$^+$ scar-associated macrophages and mesenchymal-derived cells within VML defects, with enrichment of profibrotic ligand-receptor pairs between these two populations (*106*). Myogenic cells were localized to the periphery of VML defects, suggesting that failure of tissue repair in this model could be due to an inability of these cells to migrate into the defect because of an inadequate or an inhibitory biophysical environment to support their function (*106*, *107*).

COMPARATIVE INSIGHTS FROM SPATIAL GENOMICS STUDIES ACROSS ORGANS

Continued advancements in our ability to study organ fibrosis, including now with spatial genomics approaches, have facilitated the identification of common themes linking fibrosis across organ systems while also highlighting features distinct to particular etiologies or systems (Fig. 4) (*1*, *4*).

Mapping tissue organization at the whole-organ level

The spatial context provided by spatial genomics approaches greatly complements annotation by anatomical or histological features alone (*28*, *65*, *72*, *74*, *95*, *98*, *104*). In the lung, kidney stone disease, and skeletal muscle fibrosis, where areas of fibrosis are spatially heterogeneous, spatial genomics approaches have identified transcriptomic alterations in areas deemed histologically normal (*72–75*, *98*, *99*, *103*). These findings indicate that considerable pro-fibrogenic molecular alterations can occur before discernible morphological abnormalities.

Several studies describe border or transition zones with distinct transcriptomic features and cellular constituents located between areas of normal tissue and dense fibrosis. In the liver, the perimeter of fibrosis in PSC was notable for the enrichment of transitioning cholangiocyte-like hepatocytes (*66*). In the heart, an MI border zone displaying increasing gradients of expression of *ANKRD1* and *NPPB* expression was notable (*28*), and, in the lung, emergent pathological cell populations (myofibroblasts and *KRT5*$^-$/*KRT17*$^+$ epithelial cells) with altered signaling [endoplasmic reticulum (ER) stress and wound healing] were found in transition zones containing fibroblastic foci, adjacent to areas of established fibrosis (*72*, *73*). Assessment of alterations in morphologically normal and border or transition zones thus provides opportunities to shine a light on relevant therapeutic targets earlier in the course of fibrotic disease.

Fibrotic niches or microenvironments

Key cellular processes occur in a spatially and temporally coordinated manner. Spatial genomics approaches enable researchers to define functional units as niches or microenvironments, united by gene signature and cellular composition. The emergence of fibrotic or disease-associated niches is characterized in several spatial genomics studies, often with concurrent decline in the number of healthy or homeostatic niches (*65*, *72*, *74–76*, *91*, *95*).

An example of this is in the definition of a kidney fibrotic niche. This niche is localized to the renal cortex and corticomedullary boundary and exhibited excellent correlation between ECM gene expression and histological fibrosis. A fibrotic microenvironment gene signature derived from this spatial genomics data enabled disease classification (discriminating samples with more severe disease) and accurately predicted decline in kidney function in an independent cohort of human kidney samples, demonstrating the utility of data derived using spatial genomics approaches (*91*, *95*, *96*). Several studies also identified an immune niche, resembling tertiary lymphoid structures (TLSs) in CKD, located within the fibrotic niche but with a patchy distribution (*95*, *108*). Interestingly, a similar TLS-like immune niche was identified using spatial genomics analysis of murine renal IRI (scattered throughout the kidney), human IPF, and murine bleomycin-induced lung fibrosis (*74*, *76*, *91*).

Spatial approaches also provide insight into the macroscopic organization of the fibrotic niche in relation to other niches within organs. Franzén *et al.* localized the pulmonary fibrotic niche to the periphery of fibroblastic foci, consistent with prior observations that AbBa cells are located at the "leading edge" of fibrosis (*30*, *31*, *76*). Several studies describe the association of the pulmonary fibrotic niche with distal airways, including defining an airway macrophage niche containing *SPP1*$^+$ macrophages within the lumens of these airways (*74*, *75*).

Assessment of other niches within the fibrotic organ also provides an opportunity to investigate corollary processes occurring alongside fibrosis, as evident in the context of murine skeletal muscle fibrosis

Downloaded from https://www.science.org at Shanghai Jiao Tong University on June 30, 2025

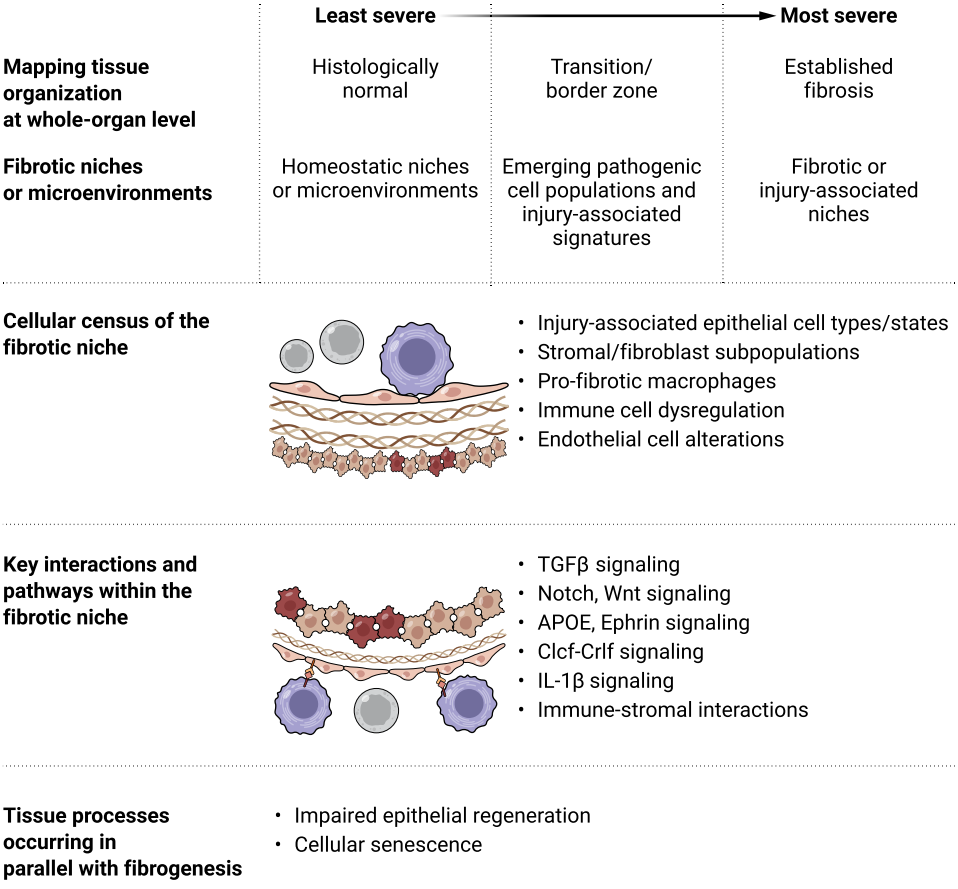
Least severe
Most severe
Mapping tissue organization at whole-organ level
Histologically normal
Transition/ border zone
Established fibrosis
Fibrotic niches or microenvironments
Homeostatic niches or microenvironments
Emerging pathogenic cell populations and injury-associated signatures
Fibrotic or injury-associated niches
Cellular census of the fibrotic niche
• Injury-associated epithelial cell types/states
• Stromal/fibroblast subpopulations
• Pro-fibrotic macrophages
• Immune cell dysregulation
• Endothelial cell alterations
Key interactions and pathways within the fibrotic niche
• TGFβ signaling
• Notch, Wnt signaling
• APOE, Ephrin signaling
• Clcf-Crlf signaling
• IL-1β signaling
• Immune-stromal interactions
Tissue processes occurring in parallel with fibrogenesis
• Impaired epithelial regeneration
• Cellular senescence

Fig. 4. Common themes arising from comparative analysis of spatial genomics studies in fibrosis. Spatial technologies allow mapping of tissue organization at a whole-organ level, complementing annotation by microanatomical and histological features. It is also possible to define functional niches or microenvironments, determining the key cellular interactions within these niches.

where distinct niches characterized by immune cell infiltration and myofiber regeneration were identified alongside the fibrotic niche (*103*). An unbiased topographical assessment of healthy organs can also aid the identification of niches susceptible to the development of fibrosis, as evidenced by the ventricular-myocardial stress niche in the heart (*10*).

Cellular census of the fibrotic niche

The composition of the fibrotic niche varies across organ systems, although subtypes of epithelial, stromal, endothelial, and immune cells are common constituents. A key feature of spatial genomics studies in lung and kidney fibrosis is the description of an injury-associated maladaptive epithelial cell type or state acting as a central hub within the fibrotic niche. In spatial genomics studies of pulmonary fibrosis, the fibrotic niche is anchored by *KRT5*$^{-}$/*KRT17*$^{+}$ AbBa cells, surrounded by fibroblasts, myofibroblasts (*CTHRC1*$^{+}$), macrophages and basal (*KRT5*$^{+}$/*KRT17*$^{+}$) and secretory airway epithelial cells (*74*–*76*). The kidney fibrotic niche is centered around *VCAM1*$^{+}$ injured proximal tubular cells (with *HAVCR1* co-expression in human kidney fibrosis) and exhibits *SPP1* and *PDGFB* expression while interacting strongly with stromal cells within the fibrotic niche (*91*, *95*, *96*, *109*). The emergence of a similar maladaptive epithelial cell state has also been described in the tall ascending limb of the loop of Henle, marked by *PROM1* and *DCD2* expression (*96*). Immune and stromal cells co-localized more frequently with injured epithelial cells in the kidney fibrotic niche (*91*, *95*–*97*).

Some commonality in fibroblast subtypes within the fibrotic niche across organs is apparent. Unsurprisingly, all organs feature a fibroblast subpopulation with a distinctive collagen synthesis or ECM signatures. Disease-associated fibroblast subpopulations are enriched for other features, including markers of stress responses, immune modulation (*CCL2*), and vascular interactions (*76*, *97*). *CCL19*$^{+}$ mesenchymal cells within the fibrotic niche are evident in both kidney and liver fibrosis (*66*, *97*), suggesting common mesenchyme-driven immune modulatory mechanisms in fibrosis in different organ systems.

Macrophages also represent a key constituent of the fibrosis-associated niche, commonly expressing *SPP1*, *TREM2*, and *CD9* (*4*, *8*, *28*, *34*, *41*, *66*, *75*, *83*). The localization of *SPP1*$^{+}$ macrophages in an airway niche adjacent to aberrant epithelial and pathogenic fibroblast populations in lung fibrosis suggests local paracrine signaling, and secreted factors from profibrotic macrophages facilitate their function in fibrosis (*76*). Notably, there was a detectable expansion of activated macrophages in the liver in PBC and an enrichment of immunosuppressive transcripts in PSC-specific monocytes, suggesting that contributions of immune cells to fibrosis may be etiology- and organ specific (*65*, *66*).

Analysis of spatially differentially expressed genes has also facilitated the identification of previously unknown cell types located outwith the fibrotic niche. In the liver, two hepatocyte populations (fibrotic Hep 1 and Hep 2) were identified, both with reduced expression of zonal markers, and the fibrotic Hep 2 population exhibited up-regulation of *CPS1* and *SCL7A2*, indicating increased capacity to metabolize ammonia in end-stage liver disease (*68*, *110*). In kidney stone disease, Canela *et al.* describe an "undifferentiated" epithelial cell cluster that localized to areas of mineralization, with a mixture of injured thin limbs and papillary epithelium signatures (*98*).

Key interactions and pathways within the fibrotic niche

Ligand-receptor interactions occurring within the fibrotic niche are influenced by the cellular constituents within the niche. Perhaps unsurprisingly, up-regulated TGFβ signaling was repeatedly observed in the spatial genomics studies discussed in this Review, in keeping with its role as a "master regulator" of fibrosis (*111*, *112*). These studies have also identified several signaling pathways involved in fibrogenesis, including EIF2 signaling (*73*), ephrin pathway (*75*), APOE signaling (*76*), IL-6 axis disruption (*72*),

CREDIT: A. FISHER/SCIENCE TRANSLATIONAL MEDICINE

Downloaded from https://www.science.org at Shanghai Jiao Tong University on June 30, 2025

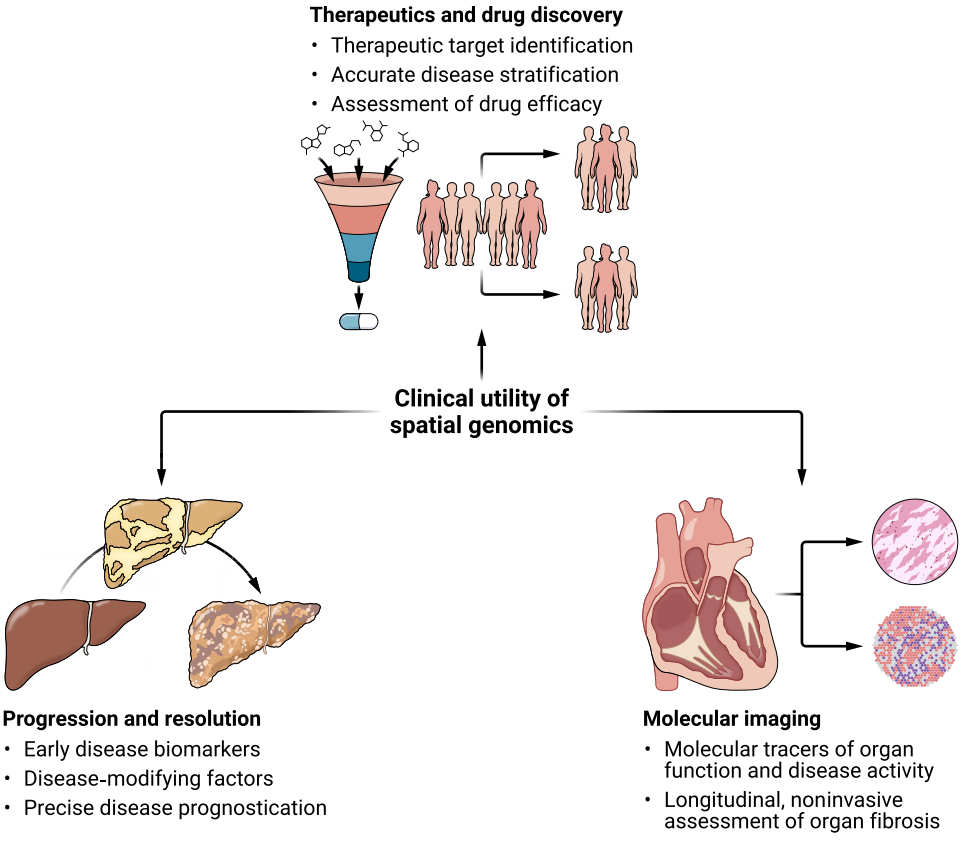
Therapeutics and drug discovery
• Therapeutic target identification
• Accurate disease stratification
• Assessment of drug efficacy
Clinical utility of spatial genomics
Progression and resolution
• Early disease biomarkers
• Disease-modifying factors
• Precise disease prognostication
Molecular imaging
• Molecular tracers of organ function and disease activity
• Longitudinal, noninvasive assessment of organ fibrosis

Fig. 5. Translating insights from spatial genomics into clinical medicine. The insights gained from spatial genomics can be leveraged toward the discovery of previously unknown therapeutics, molecular imaging tracers to aid diagnostics and prognostication, and increasing understanding of the cellular and molecular basis of fibrosis progression and resolution.

Clcf1-Crlf1 signaling (*91*), Htra3-TGFβ-IGFBP7 signaling (*84*), IL-1β–mediated macrophage-fibroblast signaling (*85*), and epidermal growth factor signaling (*96*).

Stromal-immune cross-talk is a key feature of signaling analyses in spatial genomics studies. Increased signaling (via *ADAM17* and *TGFB1*) between FAP^+ fibroblasts and phagocytic $SPP1^+CD36^+$ macrophages and $CCR2^+$ macrophages occurs after MI (*28*, *85*). A similar network between hepatic stellate cells and $SPP1^+CD36^+$ macrophages (via THBS1/2) has been demonstrated in liver fibrosis (*68*). The *CXCL12* (mesenchymal cells)/*CXCR4* (lymphocytes and myeloid cells) signaling axis in IPF, as well as kidney stromal expression of *CXCL12*, both of which mimic the microenvironment around many solid tumors, may contribute to immune suppression around the fibrotic niche (*72*, *95*, *113*). Immunoglobulin-related genes were enriched close to but not within AbBa cell–dense areas in the lung, lending weight to the theory of immune exclusion mediated by stromal cells in fibrosis (*76*). Differential expression of *CD74* by hepatic stellate cells could represent distinct antigen-presenting capabilities within this cell type (*66*, *72*).

Tissue processes occurring in parallel with fibrogenesis

The comprehensive nature of spatial genomics analyses has also facilitated the detection of biological processes occurring in parallel with fibrogenesis. In alveolar septa adjacent to fibroblastic foci, there was a notable increase in transitional AT2 cells and basal cells, indicative of alveolar remodeling and bronchiolization (*72*). A disrupted alveolar epithelial regenerative state was apparent and was linked with the progression of fibrosis in human disease, in contrast with murine experimental fibrosis where AT2 cells successfully differentiate into AT1 cells and fibrosis spontaneously regresses (*76*). Adaptive epithelial states were also localized to injury-associated niches in the kidney. Trajectory inference indicated that these cells initially interacted with immune cells and, subsequently, with the stroma, signaling a transition from inflammation to fibrosis (*96*). Modulation of epithelial regeneration may thus represent a key complementary target in the treatment of organ fibrosis.

Mayr *et al.* localized the highest degree of senescence signaling to the fibrotic niche where AbBa cells and myofibroblasts co-localize, in keeping with prior observations linking AbBa cells and senescence pathways (*30*, *31*, *75*, *78*, *114*). Injured proximal tubule epithelial cells in kidney fibrosis also exhibit a senescence-associated secretory phenotype (*95*, *96*, *109*). The accumulation of senescent cells drives fibrosis, and targeting these cells with senolytics or senomorphs represents an attractive target in organ fibrosis (*115*–*117*).

INTEGRATING SPATIAL TRANSCRIPTOMICS WITH OTHER OMICS DATA

Because the current generation of conventional spatial genomics methodologies largely produces readouts at the transcript level alone, subsequent protein-level validation is essential to establish the relevance of insights gained using these approaches. To better streamline this process, experimental technologies and computational approaches are continually being developed to seamlessly integrate spatial genomics data with other modalities beyond transcriptomics, including epigenomics, genome organization, and proteomics. Combining multi-omic information has enhanced our understanding of organ structure and function, and this has been the subject of previous comprehensive reviews (*29*, *118*). In this next section, we discuss how integrating multimodal spatial datasets furthers our understanding of fibrosis pathogenesis.

Spatial genomics and proteomics

Spatial proteomics approaches serve as a natural extension to spatial genomics approaches, especially when performed on adjacent or serial tissue segments, enabling protein validation of targets identified using spatial genomics from the same or sequential tissue sections (*119*). Methods that enable the parallel spatial interrogation of both unbiased transcriptome and proteome include spatial multiomics (*120*), a combined forerunner to 10x Genomics Visium with

CREDIT: A. FISHER/SCIENCE TRANSLATIONAL MEDICINE

Downloaded from https://www.science.org at Shanghai Jiao Tong University on June 30, 2025

DNA-barcoded antibodies. This has now been superceded by spatial protein and transcriptome sequencing (*121*), which combines Visium with polyadenylated antibody-derived tag (ADT)–conjugated antibodies, allowing for the profiling of up to 21 proteins (*120*, *121*). GeoMx DSP (NanoString) enables the quantification of both mRNA and protein abundance using ultraviolet-photocleavable linker probes or antibodies (*118*).

Imaging-based spatial genomics techniques are now limited by the number of transcripts that can be surveyed. Spatial CITE-seq uses a microfluidics-based deterministic barcoding-in-tissue approach, facilitating the mapping of the whole transcriptome with 200 to 300 proteins at 20-μm pixel resolution, the highest number of proteins to be profiled alongside the transcriptome (*122*). Other imaging-based methods, including seqFISH (*47*), MERFISH (*51*), and in situ sequencing–based (*50*) methods, are also compatible with immunofluorescence of DNA-conjugated antibodies for protein detection in the same section of tissue (*123*, *124*).

Arguably, one of the biggest benefits of combining spatial and proteomics approaches is the contemporaneous validation of RNA targets at the protein level, minimizing any signal dropout that can occur when attempting protein validation in a sequential manner and increasing the accuracy of conclusions that can be drawn from correlating mRNA and protein expression, given that they arise from the same tissue section. The scarcity of tissue sections obtained from individuals with organ fibrosis, especially from earlier in the fibrogenic process, favors methods allowing for contemporaneous readouts from fewer sections.

Spatial genomics and genome organization

Contemporaneous spatial transcriptomic and epigenetic approaches have yet to be applied to studies of organ fibrosis. Collective spatial evaluation of the transcriptome and epigenome has shed light on how epigenetic mechanisms determine cellular dynamics in tissue and transcriptional phenotype in the murine and adult brain (*125*). A similar analysis would be invaluable in improving our understanding of the epigenetic regulation of cellular populations within the multicellular fibrotic niche, identifying key targets for intervention.

Bulk epigenomics data, deconvolved into specific cell-type assignments using scRNA-seq data or single-cell assay for transposase-accessible chromatin using sequencing (ATAC-seq) data as a reference, can be used to complement spatial genomics-based data. This approach has been used to interrogate human MI and murine skin repair (*28*, *126*). Both transcriptomic and epigenetic information can also be obtained from the same tissue section, because it can be performed using spatial ATAC with RNA-seq (chromatin accessibility) and spatial cleavage under targets and tagmentation (CUT&Tag) with RNA-seq (*127*). Key considerations when using these approaches, however, are current limitations of assayable area, lack of single-cell resolution, and data loss between adjacent pixels (*122*).

Imaging-based spatial genomics approaches also allow for the concurrent measurement of the transcriptome and epigenome. Su *et al.* assessed mRNA (nascent transcripts) and chromatin (genomic loci) in the same single tissue by consecutively applying RNA-MERFISH and DNA-MERFISH, characterizing the relationship between chromatin domains, compartments, and *trans*-chromosomal interactions to transcriptional activity at single-cell resolution (*123*). This was taken a step further by Takei *et al.*, who used DNA-seqFISH$^+$ and RNA-seqFISH (70 mRNAs and nascent transcriptionally active sites of 1000 genes), in combination with antibody targeting of 17 nuclear structures to provide three layers of information from the same tissue section (*124*).

CHALLENGES AND LIMITATIONS OF CURRENT SPATIAL GENOMICS APPROACHES

The challenges and limitations and challenges of current spatial genomics approaches can be broadly categorized into technical and analytical.

Technical challenges

A key limitation of commercially available technologies is the achievable resolution. The 10x Genomics Visium platform uses slides that are coated with 55-μm-diameter oligo spots, with a 100-μm center-to-center distance. Because of the spot size, each spot encompasses a variable number of cells depending on organ and region sampled, for example, 6 to 10 cells in the liver and four cells in the heart (*28*, *65*), with unsampled tissue between these spots. To overcome the limitation of spot size, many studies have deconvolved cell-type composition within each spot using cell-type signatures derived from reference scRNA-seq or snRNA-seq atlases (*28*, *74*). Nonetheless, improvements in Visium resolution have already been achieved, with the release of Visium HD, which uses a "lawn" of 2-μm square oligos providing near–single-cell resolution and continuous tissue coverage.

Where single-cell resolution can be achieved, such as in imaging-based spatial genomics approaches, the number of transcripts that can be sequenced is limited because of the targeted application of probes in ISS- and ISH-based methods. Therefore, a compromise is often required between area of tissue studied, number of transcripts sequenced, and the resultant total amount of data generated with associated cost and time requirements for analysis.

For all commercially available platforms, a degree of optimization is required to maximize the quality of data that can be obtained, affecting the cost of experiments and requirement for tissue sections. This is particularly relevant in the context of working with dense fibrotic tissue, risking incomplete permeabilization and low RNA yield and necessitating the use of more prolonged permeabilization steps for sequencing-based approaches (*65*, *68*). This can result in the spillover of localized transcripts to adjacent areas, causing RNA content outside of capture areas and artefactual "gradients" of expression (*65*).

Analytical challenges

Computational analyses are continually being developed to allow optimal integration of spatial genomics approaches as the ability to assay multiple layers of information from the same tissue section increases. The integration of multiple data types needs to be done cautiously to minimize data loss and cope with data of varying richness, without introducing bias from the potential overreliance on reference data generated from tissue-dissociated data.

How spatial context is integrated across multiple modalities is a very active area of research and poses a considerable analytical challenge for the field, particularly in studying spatially heterogeneous fibrotic conditions such as lung fibrosis. Smoothing algorithms have been developed to help address this particular challenge, but concerns regarding batch overcorrection remain (*90*). Nonspatial single-cell approaches have benefited from concerted atlasing efforts, where the integration of large datasets generated using different modalities requires careful curation and data integration. The richness of insights

Downloaded from https://www.science.org at Shanghai Jiao Tong University on June 30, 2025

that can be obtained using a combination of different spatial genomics modalities from several different studies is obvious, with the ability to map cell position and niches using imaging-based approaches, combined with the breadth of transcriptome that can be achieved using sequencing-based approaches.

A further challenge when combining spatial genomics and dissociation-based approaches is resolving discrepancies in cell-type annotation or proportion arising from the different modalities. This has been observed in studies using liver and lung tissues (*65*, *75*). Mayr *et al.* estimated cell-type abundance per spot in Visium data of IPF lung tissue by referencing scRNA-seq data, demonstrating increased epithelial and endothelial cell fractions in spatial genomics data compared with myeloid cells, the latter of which were overrepresented in dissociation-based single-cell genomics methods (*75*). A consensus within the field may be required regarding the appropriate sample size or number of regions to be sampled per tissue section in spatial genomics–based studies (*128*). However, given the complexity and heterogeneity of pathobiology, bespoke use of spatial genomics approaches may also be required for specific research questions and disease indications.

FUTURE PERSPECTIVES IN SPATIAL GENOMICS

Technical advances in spatial genomics will further enhance the cellular resolution of sequencing-based approaches, in addition to increasing the number of transcripts captured with imaging-based approaches (*129*–*131*). Spatial transcriptomics assays will be increasingly compatible with or incorporate multiple dimensions of spatial-omics data simultaneously, greatly increasing the insights gained from individual sections of tissue. Assays that incorporate all these features are already on the horizon, such as Slide-tags, which uses spatially barcoded oligonucleotides derived from DNA-barcoded beads to label single nuclei within intact tissue that is then dissociated (*132*). Slide-tags has been further adapted to incorporate other single-cell measurement technologies, including chromatin accessibility data and T cell receptor sequences (*132*). Many of these methods will become commercially available, increasing and democratizing access to these technologies and further improving our understanding of fibrotic disease. Alongside these advances, the continued rapid development of computational analysis methods in this space will drive discovery from these rich multimodal datasets.

Translating insights from spatial genomics into clinical medicine

Clinical management of patients with organ fibrosis is hampered by delayed diagnosis, a lack of precise biomarkers, and very limited therapeutic options. Candidate therapeutics often fail in late-phase clinical trials, and the few antifibrotic therapies now approved have proven modestly effective (*133*–*135*). The reasons for this are myriad, including limitations in our understanding of both progression and regression of fibrosis as well as limited access to human tissue and the resultant reliance on imperfect in vitro and animal models of disease (*136*). However, the rich insights that will be garnered from this new wave of spatial genomics approaches should shape both our understanding of the mechanisms driving disease and the clinical management of patients with fibrosis (Fig. 4).

Diagnostics and prognostication

Fibrosis represents the end stage of a dynamic process that often evolves over many years. Clinically, patients often present late, once organ function has been substantially and irreversibly compromised. Approaches used to diagnose fibrosis in the clinic are often reliant on biochemical markers of organ dysfunction (for example, measurements of declining liver synthetic capacity, lung function, renal function, and cardiac function), overt radiological changes (detected via ultrasound or cross-sectional imaging such as computed tomography or magnetic resonance imaging), or, less commonly, tissue biopsy (often performed only in cases of diagnostic uncertainty). There is a distinct need in the field to identify biomarkers to diagnose early-stage disease, before the development of overt histological changes or clinical symptoms. Harnessing spatial genomics approaches to help identify biomarkers of early-stage and progressive disease would aid in the detection of disease in high-risk groups (improving clinical trial stratification) and could also guide prognostication after early diagnosis. Importantly, spatial genomics methodologies, by unlocking robust and precise biomarkers, could greatly facilitate noninvasive longitudinal assessment of organ fibrosis in the context of clinical trials.

There are several ways by which spatial genomics approaches can facilitate biomarker discovery. Spatial and temporal maps of fibrotic disease progression, alongside the identification of specific ligand-receptor interactions crucial to progressive fibrosis, would enable the identification of molecules directly involved in the progression of fibrosis (rather than proxy measures of organ dysfunction). Advances in spatial genomics technologies will facilitate the widespread use of formalin-fixed paraffin-embedded (FFPE) tissue samples, enabling the retrospective analysis of biobanked samples and vastly increasing our understanding of the temporal and spatial changes in gene expression occurring in fibrosis over time (*137*).

Molecular imaging

A further exciting area involves the use of spatial genomics readouts to inform the design of molecular imaging tracers (such as with positron emission tomography) to track fibrotic disease. Furthermore, tracers that target specific biomarkers of fibrotic disease could be combined with functional imaging techniques to provide a holistic, whole-organ quantitative readout of both fibrosis stage and organ function. Potentially, these tracers could be used to diagnose early disease, negating the need for biopsy, and could also be used to monitor disease progression and response to treatment (*138*).

Therapeutics

The resolution afforded by scRNA-seq in human tissue increases the likelihood of identifying tractable and disease-relevant targets (*111*). Spatial genomics studies in organ fibrosis will accelerate the discovery of effective antifibrotics by enabling the precise topographic annotation of therapeutic targets, facilitating assessment of whether the "right drug" gets to the "right target." This information can be integrated into drug development pipelines, enhancing the efficiency of candidate therapeutic compound assessment in preclinical models and clinical trials. Furthermore, accurate disease endotyping incorporating unique spatial molecular profiles will facilitate precise patient stratification, optimizing clinical trial design and outcomes. These multimodal spatial approaches will ultimately bring us closer to the personalized management of fibrotic disease in clinical practice.

CONCLUSIONS

Spatial genomics approaches are a powerful addition to the armamentarium of technologies at our disposal to interrogate organ

Downloaded from https://www.science.org at Shanghai Jiao Tong University on June 30, 2025

fibrosis. This technology has already helped illuminate distinct pathogenic cell subpopulations that are resident in fibrotic niches across organ systems and the unanticipated transcriptional perturbations present in morphologically normal tissue in fibrotic organs. These insights will undoubtedly deepen our understanding of how fibrosis initiation, progression, and regression occur.

Technical advances in spatial transcriptomics, including the ability to analyze FFPE tissue, increased resolution and transcript depth, alongside the integration of spatial transcriptomics analyses with other high-resolution omics approaches should allow a further step change in our understanding of the cellular and molecular mechanisms regulating human organ fibrosis. In the coming years, it is likely that these approaches will facilitate the development of robust biomarkers to diagnose, stage, and monitor fibrotic disease progression, and, in tandem, drive the development of effective treatments for patients with fibrosis.

REFERENCES AND NOTES

1. N. C. Henderson, F. Rieder, T. A. Wynn, Fibrosis: From mechanisms to medicines. *Nature* **587**, 555–566 (2020).
2. J. H. W. Distler, A.-H. Györfi, M. Ramanujam, M. L. Whitfield, M. Königshoff, R. Lafyatis, Shared and distinct mechanisms of fibrosis. *Nat. Rev. Rheumatol.* **15**, 705–730 (2019).
3. I. Lurje, N. T. Gaisa, R. Weiskirchen, F. Tacke, Mechanisms of organ fibrosis: Emerging concepts and implications for novel treatment strategies. *Mol. Aspects Med.* **92**, 101191 (2023).
4. M. Bhattacharya, P. Ramachandran, Immunology of human fibrosis. *Nat. Immunol.* **24**, 1423–1433 (2023).
5. M. Zhao, L. Wang, M. Wang, S. Zhou, Y. Lu, H. Cui, A. C. Racanelli, L. Zhang, T. Ye, B. Ding, B. Zhang, J. Yang, Y. Yao, Targeting fibrosis: Mechanisms and clinical trials. *Signal Transduct. Target. Ther.* **7**, 206 (2022).
6. M. J. T. Stubbington, O. Rozenblatt-Rosen, A. Regev, S. A. Teichmann, Single-cell transcriptomics to explore the immune system in health and disease. *Science* **358**, 58–63 (2017).
7. T. S. Andrews, J. Atif, J. C. Liu, C. T. Perciani, X. Z. Ma, C. Thoeni, M. Slyper, G. Eraslan, A. Segerstolpe, J. Manuel, S. Chung, E. Winter, I. Cirlan, N. Khuu, S. Fischer, O. Rozenblatt-Rosen, A. Regev, I. D. McGilvray, G. D. Bader, S. A. Macparland, Single-cell, single-nucleus, and spatial RNA sequencing of the human liver identifies cholangiocyte and mesenchymal heterogeneity. *Hepatol. Commun.* **6**, 821–840 (2022).
8. P. Ramachandran, R. Dobie, J. R. Wilson-Kanamori, E. F. Dora, B. E. P. Henderson, N. T. Luu, J. R. Portman, K. P. Matchett, M. Brice, J. A. Marwick, R. S. Taylor, M. Efremova, R. Vento-Tormo, N. O. Carragher, T. J. Kendall, J. A. Fallowfield, E. M. Harrison, D. J. Mole, S. J. Wigmore, P. N. Newsome, C. J. Weston, J. P. Iredale, F. Tacke, J. W. Pollard, C. P. Ponting, J. C. Marioni, S. A. Teichmann, N. C. Henderson, Resolving the fibrotic niche of human liver cirrhosis at single-cell level. *Nature* **575**, 512–518 (2019).
9. B. R. Conway, E. D. O'Sullivan, C. Cairns, J. O'Sullivan, D. J. Simpson, A. Salzano, K. Connor, P. Ding, D. Humphries, K. Stewart, O. Teenan, R. Pius, N. C. Henderson, C. Benezech, P. Ramachandran, D. Ferenbach, J. Hughes, T. Chandra, L. Denby, Kidney single-cell atlas reveals myeloid heterogeneity in progression and regression of kidney disease. *J. Am. Soc. Nephrol.* **31**, 2833–2854 (2020).
10. K. Kanemaru, J. Cranley, D. Muraro, A. M. A. Miranda, S. Y. Ho, A. Wilbrey-Clark, J. Patrick Pett, K. Polanski, L. Richardson, M. Litvinukova, N. Kumasaka, Y. Qin, Z. Jablonska, C. I. Semprich, L. Mach, M. Dabrowska, N. Richoz, L. Bolt, L. Mamanova, R. Kapuge, S. N. Barnett, S. Perera, C. Talavera-López, I. Mulas, K. T. Mahbubani, L. Tuck, L. Wang, M. M. Huang, M. Prete, S. Pritchard, J. Dark, K. Saeb-Parsy, M. Patel, M. R. Clatworthy, N. Hübner, R. A. Chowdhury, M. Noseda, S. A. Teichmann, Spatially resolved multiomics of human cardiac niches. *Nature* **619**, 801–810 (2023).
11. H. B. Schiller, D. T. Montoro, L. M. Simon, E. L. Rawlins, K. B. Meyer, M. Strunz, F. A. Vieira Braga, W. Timens, G. H. Koppelman, G. R. S. Budinger, J. K. Burgess, A. Waghray, M. Van Den Berge, F. J. Theis, A. Regev, N. Kaminski, J. Rajagopal, S. A. Teichmann, A. V. Misharin, M. C. Nawijn, The human lung cell atlas: A high-resolution reference map of the human lung in health and disease. *Am. J. Respir. Cell Mol. Biol.* **61**, 31–41 (2019).
12. S. Aldridge, S. A. Teichmann, Single cell transcriptomics comes of age. *Nat. Commun.* **11**, 4307 (2020).
13. A. M. A. Miranda, V. Janbandhu, H. Maatz, K. Kanemaru, J. Cranley, S. A. Teichmann, N. Hübner, M. D. Schneider, R. P. Harvey, M. Noseda, Single-cell transcriptomics for the assessment of cardiac disease. *Nat. Rev. Cardiol.* **20**, 289–308 (2023).
14. R. Elmentaite, C. D. Conde, L. Yang, S. A. Teichmann, Single-cell atlases: Shared and tissue-specific cell types across human organs. *Nat. Rev. Genet.* **23**, 395–410 (2022).
15. K. B. Halpern, I. Caspi, D. Lemze, M. Levy, S. Landen, E. Elinav, I. Ulitsky, S. Itzkovitz, Nuclear retention of mRNA in mammalian tissues. *Cell Rep.* **13**, 2653–2662 (2015).
16. G. Eraslan, E. Drokhlyansky, S. Anand, E. Fiskin, A. Subramanian, M. Slyper, J. Wang, N. Van Wittenberghe, J. M. Rouhana, J. Waldman, O. Ashenberg, M. Lek, D. Dionne, T. S. Win, M. S. Cuoco, O. Kuksenko, A. M. Tsankov, P. A. Branton, J. L. Marshall, A. Greka, G. Getz, A. V. Segrè, F. Aguet, O. Rozenblatt-Rosen, K. G. Ardlie, A. Regev, Single-nucleus cross-tissue molecular reference maps toward understanding disease gene function. *Science* **376**, eabl4290 (2022).
17. H. Wu, Y. Kirita, E. L. Donnelly, B. D. Humphreys, Advantages of single-nucleus over single-cell RNA sequencing of adult kidney: Rare cell types and novel cell states revealed in fibrosis. *J. Am. Soc. Nephrol.* **30**, 23–32 (2019).
18. M. Slyper, C. B. M. Porter, O. Ashenberg, J. Waldman, E. Drokhlyansky, I. Wakiro, C. Smillie, G. Smith-Rosario, J. Wu, D. Dionne, S. Vigneau, J. Jané-Valbuena, T. L. Tickle, S. Napolitano, M.-J. Su, A. G. Patel, A. Karlstrom, S. Gritsch, M. Nomura, A. Waghray, S. H. Gohil, A. M. Tsankov, L. Jerby-Arnon, O. Cohen, J. Klughammer, Y. Rosen, J. Gould, L. Nguyen, M. Hofree, P. J. Tramontozzi, B. Li, C. J. Wu, B. Izar, R. Haq, F. S. Hodi, C. H. Yoon, A. N. Hata, S. J. Baker, M. L. Suvà, R. Bueno, E. H. Stover, M. R. Clay, M. A. Dyer, N. B. Collins, U. A. Matulonis, N. Wagle, B. E. Johnson, A. Rotem, O. Rozenblatt-Rosen, A. Regev, A single-cell and single-nucleus RNA-Seq toolbox for fresh and frozen human tumors. *Nat. Med.* **26**, 792–802 (2020).
19. N. Thrupp, C. Sala Frigerio, L. Wolfs, N. G. Skene, N. Fattorelli, S. Poovathingal, Y. Fourne, P. M. Matthews, T. Theys, R. Mancuso, B. De Strooper, M. Fiers, Single-nucleus RNA-Seq is not suitable for detection of microglial activation genes in humans. *Cell Rep.* **32**, 108189 (2020).
20. E. Caglayan, Y. Liu, G. Konopka, Neuronal ambient RNA contamination causes misinterpreted and masked cell types in brain single-nuclei datasets. *Neuron* **110**, 4043–4056.e5 (2022).
21. A. E. Murphy, N. N. Fancy, N. G. Skene, Avoiding false discoveries in single-cell RNA-seq by revisiting the first Alzheimer's disease dataset. *eLife* **12**, RP90214 (2023).
22. A. Reichard, K. Asosingh, Best practices for preparing a single cell suspension from solid tissues for flow cytometry. *Cytometry A* **95**, 219–226 (2019).
23. A. Neuschulz, O. Bakina, V. Badillo-Lisakowski, P. Olivares-Chauvet, T. Conrad, M. Gotthardt, H. Kettenmann, J. P. Junker, A single-cell RNA labeling strategy for measuring stress response upon tissue dissociation. *Mol. Syst. Biol.* **19**, e11147 (2023).
24. E. Denisenko, B. B. Guo, M. Jones, R. Hou, L. De Kock, T. Lassmann, D. Poppe, O. Clément, R. K. Simmons, R. Lister, A. R. R. Forrest, Systematic assessment of tissue dissociation and storage biases in single-cell and single-nucleus RNA-seq workflows. *Genome Biol.* **21**, 130 (2020).
25. D. Bressan, G. Battistoni, G. J. Hannon, The dawn of spatial omics. *Science* **381**, eabq4964 (2023).
26. K. P. Matchett, J. Paris, S. A. Teichmann, N. C. Henderson, Spatial genomics: Mapping human steatotic liver disease. *Nat. Rev. Gastroenterol. Hepatol.* **21**, 646–660 (2024).
27. P. A. Reyfman, J. M. Walter, N. Joshi, K. R. Anekalla, A. C. McQuattie-Pimentel, S. Chiu, R. Fernandez, M. Akbarpour, C. I. Chen, Z. Ren, R. Verma, H. Abdala-Valencia, K. Nam, M. Chi, S. Han, F. J. Gonzalez-Gonzalez, S. Soberanes, S. Watanabe, K. J. N. Williams, A. S. Flozak, T. T. Nicholson, V. K. Morgan, D. R. Winter, M. Hinchcliff, C. L. Hrusch, R. D. Guzy, C. A. Bonham, A. I. Sperling, R. Bag, R. B. Hamanaka, G. M. Mutlu, A. V. Yeldandi, S. A. Marshall, A. Shilatifard, L. A. N. Amaral, H. Perlman, J. I. Sznajder, A. C. Argento, C. T. Gillespie, J. Dematte, M. Jain, B. D. Singer, K. M. Ridge, A. P. Lam, A. Bharat, S. M. Bhorade, C. J. Gottardi, G. R. S. Budinger, A. V. Misharin, Single-cell transcriptomic analysis of human lung provides insights into the pathobiology of pulmonary fibrosis. *Am. J. Respir. Crit. Care Med.* **199**, 1517–1536 (2019).
28. C. Kuppe, R. O. Ramirez Flores, Z. Li, S. Hayat, R. T. Levinson, X. Liao, M. T. Hannani, J. Tanevski, F. Wünnemann, J. S. Nagai, M. Halder, D. Schumacher, S. Menzel, G. Schäfer, K. Hoeft, M. Cheng, S. Ziegler, X. Zhang, F. Peisker, N. Kaesler, T. Saritas, Y. Xu, A. Kassner, J. Gummert, M. Morshuis, J. Amrute, R. J. A. Veltrop, P. Boor, K. Klingel, L. W. Van Laake, A. Vink, R. M. Hoogenboezem, E. M. J. Bindels, L. Schurgers, S. Sattler, D. Schapiro, R. K. Schneider, K. Lavine, H. Milting, I. G. Costa, J. Saez-Rodriguez, R. Kramann, Spatial multi-omic map of human myocardial infarction. *Nature* **608**, 766–777 (2022).
29. H. Li, D. Li, N. Ledru, Q. Xuanyuan, H. Wu, A. Asthana, L. N. Byers, S. G. Tullius, G. Orlando, S. S. Waikar, B. D. Humphreys, Transcriptomic, epigenomic, and spatial metabolomic cell profiling redefines regional human kidney anatomy. *Cell Metab.* **36**, 1105–1125.e10 (2024).
30. T. S. Adams, J. C. Schupp, S. Poli, E. A. Ayaub, N. Neumark, F. Ahangari, S. G. Chu, B. A. Raby, G. Deiuliis, M. Januszyk, Q. Duan, H. A. Arnett, A. Siddiqui, G. R. Washko, R. Homer, X. Yan, I. O. Rosas, N. Kaminski, Single-cell RNA-seq reveals ectopic and aberrant lung-resident cell populations in idiopathic pulmonary fibrosis. *Sci. Adv.* **6**, eaba1983 (2020).
31. A. C. Habermann, A. J. Gutierrez, L. T. Bui, S. L. Yahn, N. I. Winters, C. L. Calvi, L. Peter, M.-I. Chung, C. J. Taylor, C. Jetter, L. Raju, J. Roberson, G. Ding, L. Wood, J. M. S. Sucre, B. W. Richmond, A. P. Serezani, W. J. McDonnell, S. B. Mallal, M. J. Bacchetta, J. E. Loyd, C. M. Shaver, L. B. Ware, R. Bremner, R. Walia, T. S. Blackwell, N. E. Banovich, J. A. Kropski,

Downloaded from https://www.science.org at Shanghai Jiao Tong University on June 30, 2025

Single-cell RNA sequencing reveals profibrotic roles of distinct epithelial and mesenchymal lineages in pulmonary fibrosis. *Sci. Adv.* **6**, eaba1972 (2020).
32. R. Dobie, J. R. Wilson-Kanamori, B. E. P. Henderson, J. R. Smith, K. P. Matchett, J. R. Portman, K. Wallenborg, S. Picelli, A. Zagorska, S. V. Pendem, T. E. Hudson, M. M. Wu, G. R. Budas, D. G. Breckenridge, E. M. Harrison, D. J. Mole, S. J. Wigmore, P. Ramachandran, C. P. Ponting, S. A. Teichmann, J. C. Marioni, N. C. Henderson, Single-cell transcriptomics uncovers zonation of function in the mesenchyme during liver fibrosis. *Cell Rep.* **29**, 1832–1847.e8 (2019).
33. M. Dudek, D. Pfister, S. Donakonda, P. Filpe, A. Schneider, M. Laschinger, D. Hartmann, N. Huser, P. Meiser, F. Bayerl, D. Inverso, J. Wigger, M. Sebode, R. Ollinger, R. Rad, S. Hegenbarth, M. Anton, A. Guillot, A. Bowman, D. Heide, F. Muller, P. Ramadori, V. Leone, C. Garcia-Caceres, T. Gruber, G. Seifert, A. M. Kabat, J. P. Mallm, S. Reider, M. Effenberger, S. Roth, A. T. Billeter, B. Muller-Stich, E. J. Pearce, F. Koch-Nolte, R. Kaser, H. Tilg, R. Thimme, T. Boettler, F. Tacke, J. F. Dufour, D. Haller, P. J. Murray, R. Heeren, D. Zehn, J. P. Bottcher, M. Heikenwalder, P. A. Knolle, Auto-aggressive CXCR6^{+} CD8 T cells cause liver immune pathology in NASH. *Nature* **592**, 444–449 (2021).
34. T. Fabre, A. M. S. Barron, S. M. Christensen, S. Asano, K. Bound, M. P. Lech, M. H. Wadsworth II, X. Chen, C. Wang, J. Wang, J. McMahon, F. Schlerman, A. White, K. M. Kravarik, A. J. Fisher, L. A. Borthwick, K. M. Hart, N. C. Henderson, T. A. Wynn, K. Dower, Identification of a broadly fibrogenic macrophage subset induced by type 3 inflammation. *Sci. Immunol.* **8**, eadd8945 (2023).
35. O. Krenkel, J. Hundertmark, T. P. Ritz, R. Weiskirchen, F. Tacke, Single cell RNA sequencing identifies subsets of hepatic stellate cells and myofibroblasts in liver fibrosis. *Cells* **8**, 503 (2019).
36. T. Poch, J. Krause, C. Casar, T. Liwinski, L. Glau, M. Kaufmann, A. E. Ahrenstorf, L. U. Hess, A. E. Ziegler, G. Martrus, S. Lunemann, M. Sebode, J. Li, D. Schwinge, C. F. Krebs, A. Franke, M. A. Friese, K. J. Oldhafer, L. Fischer, M. Altfeld, A. W. Lohse, S. Huber, E. Tolosa, N. Gagliani, C. Schramm, Single-cell atlas of hepatic T cells reveals expansion of liver-resident naive-like CD4^{+} T cells in primary sclerosing cholangitis. *J. Hepatol.* **75**, 414–423 (2021).
37. J. A. Zepp, W. J. Zacharias, D. B. Frank, C. A. Cavanaugh, S. Zhou, M. P. Morley, E. E. Morrisey, Distinct mesenchymal lineages and niches promote epithelial self-renewal and myofibrogenesis in the lung. *Cell* **170**, 1134–1148.e10 (2017).
38. C. Morse, T. Tabib, J. Sembrat, K. L. Buschur, H. T. Bittar, E. Valenzi, Y. Jiang, D. J. Kass, K. Gibson, W. Chen, A. Mora, P. V. Benos, M. Rojas, R. Lafyatis, Proliferating SPP1/MERTK-expressing macrophages in idiopathic pulmonary fibrosis. *Eur. Respir. J.* **54**, 1802441 (2019).
39. K. J. Travaglini, A. N. Nabhan, L. Penland, R. Sinha, A. Gillich, R. V. Sit, S. Chang, S. D. Conley, Y. Mori, J. Seita, G. J. Berry, J. B. Shrager, R. J. Metzger, C. S. Kuo, N. Neff, I. L. Weissman, S. R. Quake, M. A. Krasnow, A molecular cell atlas of the human lung from single-cell RNA sequencing. *Nature* **587**, 619–625 (2020).
40. D. Schumacher, R. Kramann, Multiomic spatial mapping of myocardial infarction and implications for personalized therapy. *Arterioscler. Thromb. Vasc. Biol.* **43**, 192–202 (2023).
41. G. Coulis, D. Jaime, C. Guerrero-Juarez, J. M. Kastenschmidt, P. K. Farahat, Q. Nguyen, N. Pervolarakis, K. McLinden, L. Thurlow, S. Movahedi, B. S. Hughes, J. Duarte, A. Sorn, E. Montoya, I. Mozaffar, M. Dragan, S. Othy, T. Joshi, C. P. Hans, V. Kimonis, A. L. MacLean, Q. Nie, L. M. Wallace, S. Q. Harper, T. Mozaffar, M. W. Hogarth, S. Bhattacharya, J. K. Jaiswal, D. R. Golann, Q. Su, K. Kessenbrock, M. Stec, M. J. Spencer, J. R. Zamudio, S. A. Villalta, Single-cell and spatial transcriptomics identify a macrophage population associated with skeletal muscle fibrosis. *Sci. Adv.* **9**, eadd9984 (2023).
42. M. Guilliams, J. Bonnardel, B. Haest, B. Vanderborght, C. Wagner, A. Remmerie, A. Bujko, L. Martens, T. Thoné, R. Browaeys, F. F. De Ponti, B. Vanneste, C. Zwicker, F. R. Svedberg, T. Vanhalewyn, A. Gonçalves, S. Lippens, B. Devriendt, E. Cox, G. Ferrero, V. Wittamer, A. Willaert, S. J. F. Kaptein, J. Neyts, K. Dallmeier, P. Geldhof, S. Casaert, B. Deplancke, P. Ten Dijke, A. Hoorens, A. Vanlander, F. Berrevoet, Y. Van Nieuwenhove, Y. Saeys, W. Saelens, H. Van Vlierberghe, L. Devisscher, C. L. Scott, Spatial proteogenomics reveals distinct and evolutionarily conserved hepatic macrophage niches. *Cell* **185**, 379–396.e38 (2022).
43. E. Madissoon, A. J. Oliver, V. Kleshchevnikov, A. Wilbrey-Clark, K. Polanski, N. Richoz, A. Ribeiro Orsi, L. Mamanova, L. Bolt, R. Elmentaite, J. P. Pett, N. Huang, C. Xu, P. He, M. Dabrowska, S. Pritchard, L. Tuck, E. Prigmore, S. Perera, A. Knights, A. Oszlanczi, A. Hunter, S. F. Vieira, M. Patel, R. G. H. Lindeboom, L. S. Campos, K. Matsuo, T. Nakayama, M. Yoshida, K. B. Worlock, M. Z. Nikolić, N. Georgakopoulos, K. T. Mahbubani, K. Saeb-Parsy, O. A. Bayraktar, M. R. Clatworthy, O. Stegle, N. Kumasaka, S. A. Teichmann, K. B. Meyer, A spatially resolved atlas of the human lung characterizes a gland-associated immune niche. *Nat. Genet.* **55**, 66–77 (2023).
44. L. Moses, L. Pachter, Publisher correction: Museum of spatial transcriptomics. *Nat. Methods* **19**, 628 (2022).
45. S. K. Longo, M. G. Guo, A. L. Ji, P. A. Khavari, Integrating single-cell and spatial transcriptomics to elucidate intercellular tissue dynamics. *Nat. Rev. Genet.* **22**, 627–644 (2021).
46. A. Rao, D. Barkley, G. S. Franca, I. Yanai, Exploring tissue architecture using spatial transcriptomics. *Nature* **596**, 211–220 (2021).
47. P. L. Stahl, F. Salmen, S. Vickovic, A. Lundmark, J. F. Navarro, J. Magnusson, S. Giacomello, M. Asp, J. O. Westholm, M. Huss, A. Mollbrink, S. Linnarsson, S. Codeluppi, A. Borg, F. Ponten, P. I. Costea, P. Sahlen, J. Mulder, O. Bergmann, J. Lundeberg, J. Frisen, Visualization and analysis of gene expression in tissue sections by spatial transcriptomics. *Science* **353**, 78–82 (2016).
48. A. Chen, S. Liao, M. Cheng, K. Ma, L. Wu, Y. Lai, X. Qiu, J. Yang, J. Xu, S. Hao, X. Wang, H. Lu, X. Chen, X. Liu, X. Huang, Z. Li, Y. Hong, Y. Jiang, J. Peng, S. Liu, M. Shen, C. Liu, Q. Li, Y. Yuan, X. Wei, H. Zheng, W. Feng, Z. Wang, Y. Liu, Z. Wang, Y. Yang, H. Xiang, L. Han, B. Qin, P. Guo, G. Lai, P. Muñoz-Cánoves, P. H. Maxwell, J. P. Thiery, Q.-F. Wu, F. Zhao, B. Chen, M. Li, X. Dai, S. Wang, H. Kuang, J. Hui, L. Wang, J.-F. Fei, O. Wang, X. Wei, H. Lu, B. Wang, S. Liu, Y. Gu, M. Ni, W. Zhang, F. Mu, Y. Yin, H. Yang, M. Lisby, R. J. Cornall, J. Mulder, M. Uhlén, M. A. Esteban, Y. Li, L. Liu, X. Xu, J. Wang, Spatiotemporal transcriptomic atlas of mouse organogenesis using DNA nanoball-patterned arrays. *Cell* **185**, 1777–1792.e21 (2022).
49. E. Lubeck, A. F. Coskun, T. Zhiyentayev, M. Ahmad, L. Cai, Single-cell in situ RNA profiling by sequential hybridization. *Nat. Methods* **11**, 360–361 (2014).
50. R. Ke, M. Mignardi, A. Pacureanu, J. Svedlund, J. Botling, C. Wählby, M. Nilsson, In situ sequencing for RNA analysis in preserved tissue and cells. *Nat. Methods* **10**, 857–860 (2013).
51. K. H. Chen, A. N. Boettiger, J. R. Moffitt, S. Wang, X. Zhuang, Spatially resolved, highly multiplexed RNA profiling in single cells. *Science* **348**, aaa6090 (2015).
52. C. G. Williams, H. J. Lee, T. Asatsuma, R. Vento-Tormo, A. Haque, An introduction to spatial transcriptomics for biomedical research. *Genome Med.* **14**, 68 (2022).
53. J. Du, Y.-C. Yang, Z.-J. An, M.-H. Zhang, X.-H. Fu, Z.-F. Huang, Y. Yuan, J. Hou, Advances in spatial transcriptomics and related data analysis strategies. *J. Transl. Med.* **21**, 330 (2023).
54. F. P. M. Oliveira, J. M. R. S. Tavares, Medical image registration: A review. *Comput. Methods Biomech. Biomed. Engin.* **17**, 73–93 (2014).
55. S. Axelrod, M. Cai, A. Carr, J. Freeman, D. Ganguli, J. Kiggins, B. Long, T. Tung, K. Yamauchi, Starfish: Scalable pipelines for image-based transcriptomics. *J. Open Source Softw.* **6**, 2440 (2021).
56. C. Stringer, T. Wang, M. Michaelos, M. Pachitariu, Cellpose: A generalist algorithm for cellular segmentation. *Nat. Methods* **18**, 100–106 (2021).
57. V. Petukhov, R. J. Xu, R. A. Soldatov, P. Cadinu, K. Khodosevich, J. R. Moffitt, P. V. Kharchenko, Cell segmentation in imaging-based spatial transcriptomics. *Nat. Biotechnol.* **40**, 345–354 (2022).
58. X. Fu, Y. Lin, D. M. Lin, D. Mechtersheimer, C. Wang, F. Ameen, S. Ghazanfar, E. Patrick, J. Kim, J. Y. H. Yang, BIDCell: Biologically-informed self-supervised learning for segmentation of subcellular spatial transcriptomics data. *Nat. Commun.* **15**, 509 (2024).
59. Y. Zhong, X. Ren, Cell segmentation and gene imputation for imaging-based spatial transcriptomics. *bioRxiv* (2023); https://doi.org/10.1101/2023.10.26.564185.
60. F. A. Wolf, P. Angerer, F. J. Theis, SCANPY: Large-scale single-cell gene expression data analysis. *Genome Biol.* **19**, 15 (2018).
61. R. Dries, Q. Zhu, R. Dong, C.-H. L. Eng, H. Li, K. Liu, Y. Fu, T. Zhao, A. Sarkar, F. Bao, R. E. George, N. Pierson, L. Cai, G.-C. Yuan, Giotto: A toolbox for integrative analysis and visualization of spatial expression data. *Genome Biol.* **22**, 78 (2021).
62. C. Hafemeister, R. Satija, Normalization and variance stabilization of single-cell RNA-seq data using regularized negative binomial regression. *Genome Biol.* **20**, 296 (2019).
63. S. Choudhary, R. Satija, Comparison and evaluation of statistical error models for scRNA-seq. *Genome Biol.* **23**, 27 (2022).
64. V. Marx, Method of the year: Spatially resolved transcriptomics. *Nat. Methods* **18**, 9–14 (2021).
65. B. K. Chung, J. Øgaard, H. M. Reims, T. H. Karlsen, E. Melum, Spatial transcriptomics identifies enriched gene expression and cell types in human liver fibrosis. *Hepatol. Commun.* **6**, 2538–2550 (2022).
66. T. S. Andrews, D. Nakib, C. T. Perciani, X. Z. Ma, L. Liu, E. Winter, D. Camat, S. W. Chung, P. Lumanto, J. Manuel, S. Mangroo, B. Hansen, B. Arpinder, C. Thoeni, B. Sayed, J. Feld, A. Gehring, A. Gulamhusein, G. M. Hirschfield, A. Ricciuto, G. D. Bader, I. D. McGilvray, S. MacParland, Single-cell and spatial transcriptomics characterisation of the immunological landscape in the healthy and PSC human liver. *J. Hepatol.* **80**, 730–743 (2024).
67. S. Tiwari-Heckler, E. U. Yee, Y. Yalcin, J. Park, D.-H. T. Nguyen, W. Gao, E. Csizmadia, N. Afdhal, K. J. Mukamal, S. C. Robson, M. Lai, R. E. Schwartz, Z. G. Jiang, Adenosine deaminase 2 produced by infiltrative monocytes promotes liver fibrosis in nonalcoholic fatty liver disease. *Cell Rep.* **37**, 109897 (2021).
68. B. R. Watson, B. Paul, R. U. Rahman, L. Amir-Zilberstein, Å. Segerstolpe, E. T. Epstein, S. Murphy, L. Geistlinger, T. Lee, A. Shih, J. Deguine, R. J. Xavier, J. R. Moffitt, A. C. Mullen, Spatial transcriptomics of healthy and fibrotic human liver at single-cell resolution. *Nat. Commun.* **16**, 319 (2025).

Downloaded from https://www.science.org at Shanghai Jiao Tong University on June 30, 2025

69. H. Zeng, H. Qin, M. Liao, E. Zheng, X. Luo, A. Xiao, Y. Li, L. Chen, L. Wei, L. Zhao, X. Z. Ruan, P. Yang, Y. Chen, CD36 promotes de novo lipogenesis in hepatocytes through INSIG2-dependent SREBP1 processing. *Mol. Metab.* **57**, 101428 (2022).
70. P. J. Wolters, H. R. Collard, K. D. Jones, Pathogenesis of idiopathic pulmonary fibrosis. *Annu. Rev. Pathol.* **9**, 157–179 (2014).
71. D. J. Lederer, F. J. Martinez, Idiopathic pulmonary fibrosis. *N. Engl. J. Med.* **378**, 1811–1823 (2018).
72. M. Eyres, J. A. Bell, E. R. Davies, A. Fabre, A. Alzetani, S. Jogai, B. G. Marshall, D. A. Johnston, Z. Xu, S. V. Fletcher, Y. Wang, G. Marshall, D. E. Davies, E. Offer, M. G. Jones, Spatially resolved deconvolution of the fibrotic niche in lung fibrosis. *Cell Rep.* **40**, 111230 (2022).
73. R. Z. Blumhagen, J. S. Kurche, C. D. Cool, A. D. Walts, D. Heinz, T. E. Fingerlin, I. V. Yang, D. A. Schwartz, Spatially distinct molecular patterns of gene expression in idiopathic pulmonary fibrosis. *Respir. Res.* **24**, 287 (2023).
74. A. Vannan, R. Lyu, A. L. Williams, N. M. Negretti, E. D. Mee, J. Hirsh, S. Hirsh, D. S. Nichols, C. L. Calvi, C. J. Taylor, V. V. Polosukhin, A. P. Serezani, A. S. McCall, J. J. Gokey, H. Shim, L. B. Ware, M. J. Bacchetta, C. M. Shaver, T. S. Blackwell, R. Walia, J. M. Sucre, J. A. Kropski, D. J. McCarthy, N. E. Banovich, Image-based spatial transcriptomics identifies molecular niche dysregulation associated with distal lung remodeling in pulmonary fibrosis. bioRxiv (2023); https://doi.org/10.1101/2023.12.15.571954.
75. C. H. Mayr, D. Santacruz, S. Jarosch, M. Bleck, J. Dalton, A. McNabola, C. Lempp, L. Neubert, B. Rath, J. C. Kamp, D. Jonigk, M. Kühnel, H. Schlüter, A. Klimowicz, J. Doerr, A. Dick, F. Ramirez, M. J. Thomas, Spatial transcriptomic characterization of pathologic niches in IPF. *Sci. Adv.* **10**, eadl5473 (2024).
76. L. Franzén, M. Olsson Lindvall, M. Hühn, V. Ptasinski, L. Setyo, B. P. Keith, A. Collin, S. Oag, T. Volckaert, A. Borde, J. Lundeberg, J. Lindgren, G. Belfield, S. Jackson, A. Ollerstam, M. Stamou, P. L. Ståhl, J. J. Hornberg, Mapping spatially resolved transcriptomes in human and mouse pulmonary fibrosis. *Nat. Genet.* **56**, 1725–1736 (2024).
77. L. Franzén, M. O. Lindvall, M. Hühn, V. Ptasinski, L. Setyo, B. P. Keith, A. Collin, S. Oag, T. Volckaert, A. Borde, J. Lundeberg, J. Lindgren, G. Belfield, S. Jackson, A. Ollerstam, M. Stamou, P. L. Ståhl, J. J. Hornberg, Mapping the lung fibrosis transcriptome of mice and men. *Nat. Genet.* **56**, 1550–1551 (2024).
78. M. Strunz, L. M. Simon, M. Ansari, J. J. Kathiriya, I. Angelidis, C. H. Mayr, G. Tsidiridis, M. Lange, L. F. Mattner, M. Yee, P. Ogar, A. Sengupta, I. Kukhtevich, R. Schneider, Z. Zhao, C. Voss, T. Stoeger, J. H. L. Neumann, A. Hilgendorff, J. Behr, M. O'Reilly, M. Lehmann, G. Burgstaller, M. Königshoff, H. A. Chapman, F. J. Theis, H. B. Schiller, Alveolar regeneration through a Krt8+ transitional stem cell state that persists in human lung fibrosis. *Nat. Commun.* **11**, 3559 (2020).
79. M. A. Seibold, A. L. Wise, M. C. Speer, M. P. Steele, K. K. Brown, J. E. Loyd, T. E. Fingerlin, W. Zhang, G. Gudmundsson, S. D. Groshong, C. M. Evans, S. Garantziotis, K. B. Adler, B. F. Dickey, R. M. Du Bois, I. V. Yang, A. Herron, D. Kervitsky, J. L. Talbert, C. Markin, J. Park, A. L. Crews, S. H. Slifer, S. Auerbach, M. G. Roy, J. Lin, C. E. Hennessy, M. I. Schwarz, D. A. Schwartz, A common MUC5B promoter polymorphism and pulmonary fibrosis. *N. Engl. J. Med.* **364**, 1503–1512 (2011).
80. J. S. Kurche, C. D. Cool, R. Z. Blumhagen, E. Dobrinskikh, D. Heinz, J. A. Herrera, I. V. Yang, D. A. Schwartz, *MUC5B* idiopathic pulmonary fibrosis risk variant promotes a mucosecretory phenotype and loss of small airway secretory cells. *Am. J. Respir. Crit. Care Med.* **210**, 517–521 (2024).
81. F. Kruse, J. P. Junker, A. Van Oudenaarden, J. Bakkers, Tomo-seq: A method to obtain genome-wide expression data with spatial resolution. *Methods Cell Biol.* **135**, 299–307 (2016).
82. G. P. A. Lacraz, J. P. Junker, M. M. Gladka, B. Molenaar, K. T. Scholman, M. Vigil-Garcia, D. Versteeg, H. De Ruiter, M. W. Vermunt, M. P. Creyghton, M. M. H. Huibers, N. De Jonge, A. Van Oudenaarden, E. Van Rooij, Tomo-seq identifies SOX9 as a key regulator of cardiac fibrosis during ischemic injury. *Circulation* **136**, 1396–1409 (2017).
83. S.-H. Jung, B.-H. Hwang, S. Shin, E.-H. Park, S.-H. Park, C. W. Kim, E. Kim, E. Choo, I. J. Choi, F. K. Swirski, K. Chang, Y.-J. Chung, Spatiotemporal dynamics of macrophage heterogeneity and a potential function of Trem2^{hi} macrophages in infarcted hearts. *Nat. Commun.* **13**, 4580 (2022).
84. T. Ko, S. Nomura, S. Yamada, K. Fujita, T. Fujita, M. Satoh, C. Oka, M. Katoh, M. Ito, M. Katagiri, T. Sassa, B. Zhang, S. Hatsuse, T. Yamada, M. Harada, H. Toko, E. Amiya, M. Hatano, O. Kinoshita, K. Nawata, H. Abe, T. Ushiku, M. Ono, M. Ikeuchi, H. Morita, H. Aburatani, I. Komuro, Cardiac fibroblasts regulate the development of heart failure via Htra3-TGF-β-IGFBP7 axis. *Nat. Commun.* **13**, 3275 (2022).
85. J. M. Amrute, X. Luo, V. Penna, A. Bredemeyer, T. Yamawaki, G. S. Heo, S. Shi, A. Koenig, S. Yang, F. Kadyrov, C. Jones, C. Kuppe, B. Kopecky, S. Hayat, P. Ma, G. Feng, Y. Terada, A. Fu, M. Furtado, D. Kreisel, N. O. Stitziel, C.-M. Li, R. Kramann, Y. Liu, B. Ason, K. J. Lavine, Targeting the immune-fibrosis axis in myocardial infarction and heart failure. bioRxiv (2022); https://doi.org/10.1101/2022.10.17.512579.
86. M. Stoeckius, C. Hafemeister, W. Stephenson, B. Houck-Loomis, P. K. Chattopadhyay, H. Swerdlow, R. Satija, P. Smibert, Simultaneous epitope and transcriptome measurement in single cells. *Nat. Methods* **14**, 865–868 (2017).
87. P. Romagnani, G. Remuzzi, R. Glassock, A. Levin, K. J. Jager, M. Tonelli, Z. Massy, C. Wanner, H.-J. Anders, Chronic kidney disease. *Nat. Rev. Dis. Primers.* **3**, 17088 (2017).
88. E. Ó. Hainmhire, B. D. Humphreys, Fibrotic changes mediating acute kidney injury to chronic kidney disease transition. *Nephron* **137**, 264–267 (2017).
89. S. Djudjaj, P. Boor, Cellular and molecular mechanisms of kidney fibrosis. *Mol. Aspects Med.* **65**, 16–36 (2019).
90. E. E. Dixon, H. Wu, Y. Muto, P. C. Wilson, B. D. Humphreys, Spatially resolved transcriptomic analysis of acute kidney injury in a female murine model. *J. Am. Soc. Nephrol.* **33**, 279–289 (2022).
91. M. Polonsky, L. M. S. Gerhardt, J. Yun, K. Koppitch, K. L. Colón, H. Amrhein, S. Zheng, G.-C. Yuan, M. Thomson, L. Cai, A. P. McMahon, Spatial transcriptomics defines injury-specific microenvironments in the adult mouse kidney and novel cellular interactions in regeneration and disease. bioRxiv (2023); https://doi.org/10.1101/2023.11.22.568217.
92. M. Murakami, D. Kamimura, T. Hirano, Pleiotropy and specificity: Insights from the interleukin 6 family of cytokines. *Immunity* **50**, 812–831 (2019).
93. D. A. Ferenbach, J. V. Bonventre, Mechanisms of maladaptive repair after AKI leading to accelerated kidney ageing and CKD. *Nat. Rev. Nephrol.* **11**, 264–276 (2015).
94. Y. Kirita, H. Wu, K. Uchimura, P. C. Wilson, B. D. Humphreys, Cell profiling of mouse acute kidney injury reveals conserved cellular responses to injury. *Proc. Natl. Acad. Sci. U.S.A.* **117**, 15874–15883 (2020).
95. A. Abedini, J. Levinsohn, K. A. Klötzer, B. Dumoulin, Z. Ma, J. Frederick, P. Dhillon, M. S. Balzer, R. Shrestha, H. Liu, S. Vitale, A. M. Bergeson, K. Devalaraja-Narashimha, P. Grandi, T. Bhattacharyya, E. Hu, S. S. Pullen, C. M. Boustany-Kari, P. Guarnieri, A. Karihaloo, D. Traum, H. Yan, K. Coleman, M. Palmer, L. Sarov-Blat, L. Morton, C. A. Hunter, K. H. Kaestner, M. Li, K. Susztak, Single-cell multi-omic and spatial profiling of human kidneys implicates the fibrotic microenvironment in kidney disease progression. *Nat. Genet.* **56**, 1712–1724 (2024).
96. B. B. Lake, R. Menon, S. Winfree, Q. Hu, R. M. Ferreira, K. Kalhor, D. Barwinska, E. A. Otto, M. Ferkowicz, D. Diep, N. Plongthongkum, A. Knoten, S. Urata, L. H. Mariani, A. S. Naik, S. Eddy, B. Zhang, Y. Wu, D. Salamon, J. C. Williams, X. Wang, K. S. Balderrama, P. J. Hoover, E. Murray, J. L. Marshall, T. Noel, A. Vijayan, A. Hartman, F. Chen, S. S. Waikar, S. E. Rosas, F. P. Wilson, P. M. Palevsky, K. Kiryluk, J. R. Sedor, R. D. Toto, C. R. Parikh, E. H. Kim, R. Satija, A. Greka, E. Z. Macosko, P. V. Kharchenko, J. P. Gaut, J. B. Hodgin, KPMP Consortium, M. T. Eadon, P. C. Dagher, T. M. El-Achkar, K. Zhang, M. Kretzler, S. Jain, An atlas of healthy and injured cell states and niches in the human kidney. *Nature* **619**, 585–594 (2023).
97. D. Chen, M. Shao, Y. Song, G. Ren, F. Guo, X. Fan, Y. Wang, W. Zhang, G. Qin, Single-cell RNA seq with spatial transcriptomics to create an atlas of human diabetic kidney disease. *FASEB J.* **37**, e22938 (2023).
98. V. H. Canela, W. S. Bowen, R. M. Ferreira, F. Syed, J. E. Lingeman, A. R. Sabo, D. Barwinska, S. Winfree, B. B. Lake, Y.-H. Cheng, J. P. Gaut, M. Ferkowicz, K. A. Lafavers, K. Zhang, F. L. Coe, E. Worcester, S. Jain, M. T. Eadon, J. C. Williams, T. M. El-Achkar, A spatially anchored transcriptomic atlas of the human kidney papilla identifies significant immune injury in patients with stone disease. *Nat. Commun.* **14**, 4140 (2023).
99. G. Clair, H. Soloyan, P. Cravedi, A. Angeletti, F. Salem, L. Al-Rabadi, R. E. De Filippo, S. Da Sacco, K. V. Lemley, S. Sedrakyan, L. Perin, The spatially resolved transcriptome signatures of glomeruli in chronic kidney disease. *JCI Insight* **9**, e165515 (2024).
100. C. A. Gadegbeku, D. S. Gipson, L. B. Holzman, A. O. Ojo, P. X. K. Song, L. Barisoni, M. G. Sampson, J. B. Kopp, K. V. Lemley, P. J. Nelson, C. C. Lienczewski, S. G. Adler, G. B. Appel, D. C. Cattran, M. J. Choi, G. Contreras, K. M. Dell, F. C. Fervenza, K. L. Gibson, L. A. Greenbaum, J. D. Hernandez, S. M. Hewitt, S. R. Hingorani, M. Hladunewich, M. C. Hogan, S. L. Hogan, F. J. Kaskel, J. C. Lieske, K. E. C. Meyers, P. H. Nachman, C. C. Nast, A. M. Neu, H. N. Reich, J. R. Sedor, C. B. Sethna, H. Trachtman, K. R. Tuttle, O. Zhdanova, G. E. Zilleruelo, M. Kretzler, Design of the Nephrotic Syndrome Study Network (NEPTUNE) to evaluate primary glomerular nephropathy by a multidisciplinary approach. *Kidney Int.* **83**, 749–756 (2013).
101. C. J. Mann, E. Perdiguero, Y. Kharraz, S. Aguilar, P. Pessina, A. L. Serrano, P. Muñoz-Cánoves, Aberrant repair and fibrosis development in skeletal muscle. *Skelet. Muscle* **1**, 21 (2011).
102. D. W. Hammers, C. C. Hart, M. K. Matheny, L. A. Wright, M. Armellini, E. R. Barton, H. L. Sweeney, The D2.mdx mouse as a preclinical model of the skeletal muscle pathology associated with Duchenne muscular dystrophy. *Sci. Rep.* **10**, 14070 (2020).
103. M. J. Stec, Q. Su, C. Adler, L. Zhang, D. R. Golann, N. P. Khan, L. Panagis, S. A. Villalta, M. Ni, Y. Wei, J. R. Walls, A. J. Murphy, G. D. Yancopoulos, G. S. Atwal, S. Kleiner, G. Halasz, M. W. Sleeman, A cellular and molecular spatial atlas of dystrophic muscle. *Proc. Natl. Acad. Sci. U.S.A.* **120**, e2221249120 (2023).
104. L. G. M. Heezen, T. Abdelaal, M. Van Putten, A. Aartsma-Rus, A. Mahfouz, P. Spitali, Spatial transcriptomics reveal markers of histopathological changes in Duchenne muscular dystrophy mouse models. *Nat. Commun.* **14**, 4909 (2023).
105. J. Larouche, S. M. Greising, B. T. Corona, C. A. Aguilar, Robust inflammatory and fibrotic signaling following volumetric muscle loss: A barrier to muscle regeneration. *Cell Death Dis.* **9**, 409 (2018).

Downloaded from https://www.science.org at Shanghai Jiao Tong University on June 30, 2025

106. J. A. Larouche, E. C. Wallace, B. D. Spence, E. Buras, C. A. Aguilar, Spatiotemporal mapping of immune and stem cell dysregulation after volumetric muscle loss. *JCI Insight* **8**, e162835 (2023).
107. M. Loreti, A. Sacco, The jam session between muscle stem cells and the extracellular matrix in the tissue microenvironment. *NPJ Regen. Med.* **7**, 16 (2022).
108. Y. Sato, K. Silina, M. Van Den Broek, K. Hirahara, M. Yanagita, The roles of tertiary lymphoid structures in chronic diseases. *Nat. Rev. Nephrol.* **19**, 525–537 (2023).
109. L. M. S. Gerhardt, J. Liu, K. Koppitch, P. E. Cippà, A. P. McMahon, Single-nuclear transcriptomics reveals diversity of proximal tubule cell states in a dynamic response to acute kidney injury. *Proc. Natl. Acad. Sci. U.S.A.* **118**, e2026684118 (2021).
110. J. Paris, N. C. Henderson, Liver zonation, revisited. *Hepatology* **76**, 1219–1230 (2022).
111. X.-M. Meng, D. J. Nikolic-Paterson, H. Y. Lan, TGF-β: The master regulator of fibrosis. *Nat. Rev. Nephrol.* **12**, 325–338 (2016).
112. N. G. Frangogiannis, Transforming growth factor–β in tissue fibrosis. *J. Exp. Med.* **217**, e20190103 (2020).
113. C. Feig, J. O. Jones, M. Kraman, R. J. B. Wells, A. Deonarine, D. S. Chan, C. M. Connell, E. W. Roberts, Q. Zhao, O. L. Caballero, S. A. Teichmann, T. Janowitz, D. I. Jodrell, D. A. Tuveson, D. T. Fearon, Targeting CXCL12 from FAP-expressing carcinoma-associated fibroblasts synergizes with anti–PD-L1 immunotherapy in pancreatic cancer. *Proc. Natl. Acad. Sci. U.S.A.* **110**, 20212–20217 (2013).
114. Y. Kobayashi, A. Tata, A. Konkimalla, H. Katsura, R. F. Lee, J. Ou, N. E. Banovich, J. A. Kropski, P. R. Tata, Persistence of a regeneration-associated, transitional alveolar epithelial cell state in pulmonary fibrosis. *Nat. Cell Biol.* **22**, 934–946 (2020).
115. M. J. Schafer, T. A. White, K. Iijima, A. J. Haak, G. Ligresti, E. J. Atkinson, A. L. Oberg, J. Birch, H. Salmonowicz, Y. Zhu, D. L. Mazula, R. W. Brooks, H. Fuhrmann-Stroissnigg, T. Pirtskhalava, Y. S. Prakash, T. Tchkonia, P. D. Robbins, M. C. Aubry, J. F. Passos, J. L. Kirkland, D. J. Tschumperlin, H. Kita, N. K. Lebrasseur, Cellular senescence mediates fibrotic pulmonary disease. *Nat. Commun.* **8**, 14532 (2017).
116. K. J. Mylonas, E. D. O'Sullivan, D. Humphries, D. P. Baird, M.-H. Docherty, S. A. Neely, P. J. Krimpenfort, A. Melk, R. Schmitt, S. Ferreira-Gonzalez, S. J. Forbes, J. Hughes, D. A. Ferenbach, Cellular senescence inhibits renal regeneration after injury in mice, with senolytic treatment promoting repair. *Sci. Transl. Med.* **13**, eabb0203 (2021).
117. S. O'Reilly, P.-S. Tsou, J. Varga, Senescence and tissue fibrosis: Opportunities for therapeutic targeting. *Trends Mol. Med.* **30**, 1113–1125 (2024).
118. K. Vandereyken, A. Sifrim, B. Thienpont, T. Voet, Methods and applications for single-cell and spatial multi-omics. *Nat. Rev. Genet.* **24**, 494–515 (2023).
119. A. Baysoy, Z. Bai, R. Satija, R. Fan, The technological landscape and applications of single-cell multi-omics. *Nat. Rev. Mol. Cell Biol.* **24**, 695–713 (2023).
120. S. Vickovic, B. Lötstedt, J. Klughammer, S. Mages, Å. Segerstolpe, O. Rozenblatt-Rosen, A. Regev, SM-Omics is an automated platform for high-throughput spatial multi-omics. *Nat. Commun.* **13**, 795 (2022).
121. N. Ben-Chetrit, X. Niu, A. D. Swett, J. Sotelo, M. S. Jiao, C. M. Stewart, C. Potenski, P. Mielinis, P. Roelli, M. Stoeckius, D. A. Landau, Integration of whole transcriptome spatial profiling with protein markers. *Nat. Biotechnol.* **41**, 788–793 (2023).
122. Y. Liu, M. Distasio, G. Su, H. Asashima, A. Enninful, X. Qin, Y. Deng, P. Bordignon, M. Cassano, M. Tomayko, M. Xu, S. Halene, J. E. Craft, D. Hafler, R. Fan, Spatial-CITE-seq: spatially resolved high-plex protein and whole transcriptome co-mapping, Research Square [Preprint] (2022); https://www.researchsquare.com/article/rs-1499315/v1.
123. J.-H. Su, P. Zheng, S. S. Kinrot, B. Bintu, X. Zhuang, Genome-scale imaging of the 3D organization and transcriptional activity of chromatin. *Cell* **182**, 1641–1659.e26 (2020).
124. Y. Takei, J. Yun, S. Zheng, N. Ollikainen, N. Pierson, J. White, S. Shah, J. Thomassie, S. Suo, C.-H. L. Eng, M. Guttman, G.-C. Yuan, L. Cai, Integrated spatial genomics reveals global architecture of single nuclei. *Nature* **590**, 344–350 (2021).
125. D. Zhang, Y. Deng, P. Kukanja, E. Agirre, M. Bartosovic, M. Dong, C. Ma, S. Ma, G. Su, S. Bao, Y. Liu, Y. Xiao, G. B. Rosoklija, A. J. Dwork, J. J. Mann, K. W. Leong, M. Boldrini, L. Wang, M. Haeussler, B. J. Raphael, Y. Kluger, G. Castelo-Branco, R. Fan, Spatial epigenome–transcriptome co-profiling of mammalian tissues. *Nature* **616**, 113–122 (2023).
126. D. S. Foster, M. Januszyk, K. E. Yost, M. S. Chinta, G. S. Gulati, A. T. Nguyen, A. R. Burcham, A. Salhotra, R. C. Ransom, D. Henn, K. Chen, S. Mascharak, K. Tolentino, A. L. Titan, R. E. Jones, O. Da Silva, W. T. Leavitt, C. D. Marshall, H. E. D. Jardins-Park, M. S. Hu, D. C. Wan, G. Wernig, D. Wagh, J. Coller, J. A. Norton, G. C. Gurtner, A. M. Newman, H. Y. Chang, M. T. Longaker, Integrated spatial multiomics reveals fibroblast fate during tissue repair. *Proc. Natl. Acad. Sci. U.S.A.* **118**, e2110025118 (2021).
127. Y. Deng, M. Bartosovic, S. Ma, D. Zhang, P. Kukanja, Y. Xiao, G. Su, Y. Liu, X. Qin, G. B. Rosoklija, A. J. Dwork, J. J. Mann, M. L. Xu, S. Halene, J. E. Craft, K. W. Leong, M. Boldrini, G. Castelo-Branco, R. Fan, Spatial profiling of chromatin accessibility in mouse and human tissues. *Nature* **609**, 375–383 (2022).
128. M. Ryaboshapkina, V. Azzu, Sample size calculation for a NanoString GeoMx spatial transcriptomics experiment to study predictors of fibrosis progression in non-alcoholic fatty liver disease. *Sci. Rep.* **13**, 8943 (2023).
129. M. Nagendran, J. Sapida, J. Arthur, Y. Yin, S. D. Tuncer, N. Anaparthy, A. Gupta, M. Serra, D. Patterson, A. Tentori, 1457 Visium HD enables spatially resolved, single-cell scale resolution mapping of FFPE human breast cancer tissue. *J. Immunother. Cancer* **11**, 10.1136/jitc-2023-SITC2023.1457 (2023).
130. A. Janesick, R. Shelansky, A. D. Gottscho, F. Wagner, S. R. Williams, M. Rouault, G. Beliakoff, C. A. Morrison, M. F. Oliveira, J. T. Sicherman, A. Kohlway, J. Abousoud, T. Y. Drennon, S. H. Mohabbat, S. E. B. Taylor, High resolution mapping of the tumor microenvironment using integrated single-cell, spatial and in situ analysis. *Nat. Commun.* **14**, 8353 (2023).
131. S. He, R. Bhatt, C. Brown, E. A. Brown, D. L. Buhr, K. Chantranuvatana, P. Danaher, D. Dunaway, R. G. Garrison, G. Geiss, M. T. Gregory, M. L. Hoang, R. Khafizov, E. E. Killingbeck, D. Kim, T. K. Kim, Y. Kim, A. Klock, M. Korukonda, A. Kutchma, Z. R. Lewis, Y. Liang, J. S. Nelson, G. T. Ong, E. P. Perillo, J. C. Phan, T. Phan-Everson, E. Piazza, T. Rane, Z. Reitz, M. Rhodes, A. Rosenbloom, D. Ross, H. Sato, A. W. Wardhani, C. A. Williams-Wietzikoski, L. Wu, J. M. Beechem, High-plex imaging of RNA and proteins at subcellular resolution in fixed tissue by spatial molecular imaging. *Nat. Biotechnol.* **40**, 1794–1806 (2022).
132. A. J. C. Russell, J. A. Weir, N. M. Nadaf, M. Shabet, V. Kumar, S. Kambhampati, R. Raichur, G. J. Marrero, S. Liu, K. S. Balderrama, C. R. Vanderburg, V. Shanmugam, L. Tian, J. B. Iorgulescu, C. H. Yoon, C. J. Wu, E. Z. Macosko, F. Chen, Slide-tags enables single-nucleus barcoding for multimodal spatial genomics. *Nature* **625**, 101–109 (2024).
133. B. A. Karimi-Shah, B. A. Chowdhury, Forced vital capacity in idiopathic pulmonary fibrosis—FDA review of pirfenidone and nintedanib. *N. Engl. J. Med.* **372**, 1189–1191 (2015).
134. A. J. Podolanczuk, L. Richeldi, F. J. Martinez, The future of clinical trials in idiopathic pulmonary fibrosis. *JAMA* **329**, 1554 (2023).
135. S. A. Harrison, A. M. Allen, J. Dubourg, M. Noureddin, N. Alkhouri, Challenges and opportunities in NASH drug development. *Nat. Med.* **29**, 562–573 (2023).
136. P. N. Brennan, A. M. Elsharkawy, T. J. Kendall, R. Loomba, D. A. Mann, J. A. Fallowfield, Antifibrotic therapy in nonalcoholic steatohepatitis: Time for a human-centric approach. *Nat. Rev. Gastroenterol. Hepatol.* **20**, 679–688 (2023).
137. E. Gracia Villacampa, L. Larsson, R. Mirzazadeh, L. Kvastad, A. Andersson, A. Mollbrink, G. Kokaraki, V. Monteil, N. Schultz, K. S. Appelberg, N. Montserrat, H. Zhang, J. M. Penninger, W. Miesbach, A. Mirazimi, J. Carlson, J. Lundeberg, Genome-wide spatial expression profiling in formalin-fixed tissues. *Cell Genomics* **1**, 100065 (2021).
138. J. Bussink, J. H. A. M. Kaanders, W. T. A. Van Der Graaf, W. J. G. Oyen, PET–CT for radiotherapy treatment planning and response monitoring in solid tumors. *Nat. Rev. Clin. Oncol.* **8**, 233–242 (2011).
139. E. Zhao, M. R. Stone, X. Ren, J. Guenthoer, K. S. Smythe, T. Pulliam, S. R. Williams, C. R. Uytingco, S. E. B. Taylor, P. Nghiem, J. H. Bielas, R. Gottardo, Spatial transcriptomics at subspot resolution with BayesSpace. *Nat. Biotechnol.* **39**, 1375–1384 (2021).
140. L. Bergenstråhle, B. He, J. Bergenstråhle, X. Abalo, R. Mirzazadeh, K. Thrane, A. L. Ji, A. Andersson, L. Larsson, N. Stakenborg, G. Boeckxstaens, P. Khavari, J. Zou, J. Lundeberg, J. Maaskola, Super-resolved spatial transcriptomics by deep data fusion. *Nat. Biotechnol.* **40**, 476–479 (2022).
141. D. Pham, X. Tan, B. Balderson, J. Xu, L. F. Grice, S. Yoon, E. F. Willis, M. Tran, P. Y. Lam, A. Raghubar, P. Kalita-De Croft, S. Lakhani, J. Vukovic, M. J. Ruitenberg, Q. H. Nguyen, Robust mapping of spatiotemporal trajectories and cell–cell interactions in healthy and diseased tissues. *Nat. Commun.* **14**, 1–26 (2023).
142. V. Svensson, S. A. Teichmann, O. Stegle, SpatialDE: Identification of spatially variable genes. *Nat. Methods* **15**, 343–346 (2018).
143. L. Larsson, L. Franzén, P. L. Ståhl, J. Lundeberg, *Semla*: A versatile toolkit for spatially resolved transcriptomics analysis and visualization. *Bioinformatics* **39**, btad626 (2023).
144. S. G. Rodriques, R. R. Stickels, A. Goeva, C. A. Martin, E. Murray, C. R. Vanderburg, J. Welch, L. M. Chen, F. Chen, E. Z. Macosko, Slide-seq: A scalable technology for measuring genome-wide expression at high spatial resolution. *Science* **363**, 1463–1467 (2019).
145. M. Elosua-Bayes, P. Nieto, E. Mereu, I. Gut, H. Heyn, SPOTlight: Seeded NMF regression to deconvolute spatial transcriptomics spots with single-cell transcriptomes. *Nucleic Acids Res.* **49**, e50 (2021).
146. D. M. Cable, E. Murray, L. S. Zou, A. Goeva, E. Z. Macosko, F. Chen, R. A. Irizarry, Robust decomposition of cell type mixtures in spatial transcriptomics. *Nat. Biotechnol.* **40**, 517–526 (2022).
147. V. Kleshchevnikov, A. Shmatko, E. Dann, A. Aivazidis, H. W. King, T. Li, R. Elmentaite, A. Lomakin, V. Kedlian, A. Gayoso, M. S. Jain, J. S. Park, L. Ramona, E. Tuck, A. Arutyunyan, R. Vento-Tormo, M. Gerstung, L. James, O. Stegle, O. A. Bayraktar, Cell2location maps fine-grained cell types in spatial transcriptomics. *Nat. Biotechnol.* **40**, 661–671 (2022).
148. T. Biancalani, G. Scalia, L. Buffoni, R. Avasthi, Z. Lu, A. Sanger, N. Tokcan, C. R. Vanderburg, Å. Segerstolpe, M. Zhang, I. Avraham-Davidi, S. Vickovic, M. Nitzan, S. Ma, A. Subramanian, M. Lipinski, J. Buenrostro, N. B. Brown, D. Fanelli, X. Zhuang, E. Z. Macosko, A. Regev, Deep learning and alignment of spatially resolved single-cell transcriptomes with Tangram. *Nat. Methods* **18**, 1352–1362 (2021).

Downloaded from https://www.science.org at Shanghai Jiao Tong University on June 30, 2025

149. R. Lopez, B. Li, H. Keren-Shaul, P. Boyeau, M. Kedmi, D. Pilzer, A. Jelinski, I. Yofe, E. David, A. Wagner, C. Ergen, Y. Addadi, O. Golani, F. Ronchese, M. I. Jordan, I. Amit, N. Yosef, DestVI identifies continuums of cell types in spatial transcriptomics data. *Nat. Biotechnol.* **40**, 1360–1369 (2022).
150. Y. Hao, T. Stuart, M. H. Kowalski, S. Choudhary, P. Hoffman, A. Hartman, A. Srivastava, G. Molla, S. Madad, C. Fernandez-Granda, R. Satija, Dictionary learning for integrative, multimodal and scalable single-cell analysis. *Nat. Biotechnol.* **42**, 293–304 (2024).
151. Z. Cang, Q. Nie, Inferring spatial and signaling relationships between cells from single cell transcriptomic data. *Nat. Commun.* **11**, 2084 (2020).
152. E. Armingol, H. M. Baghdassarian, C. Martino, A. Perez-Lopez, C. Aamodt, R. Knight, N. E. Lewis, Context-aware deconvolution of cell–cell communication with Tensor-cell2cell. *Nat. Commun.* **13**, 3665 (2022).
153. J. Tanevski, R. O. R. Flores, A. Gabor, D. Schapiro, J. Saez-Rodriguez, Explainable multiview framework for dissecting spatial relationships from highly multiplexed data. *Genome Biol.* **23**, 97 (2022).
154. L. Garcia-Alonso, L.-F. Handfield, K. Roberts, K. Nikolakopoulou, R. C. Fernando, L. Gardner, B. Woodhams, A. Arutyunyan, K. Polanski, R. Hoo, C. Sancho-Serra, T. Li, K. Kwakwa, E. Tuck, V. Lorenzi, H. Massalha, M. Prete, V. Kleshchevnikov, A. Tarkowska, T. Porter, C. I. Mazzeo, S. Van Dongen, M. Dabrowska, V. Vaskivskyi, K. T. Mahbubani, J.-E. Park, M. Jimenez-Linan, L. Campos, V. Y. Kiselev, C. Lindskog, P. Ayuk, E. Prigmore, M. R. Stratton, K. Saeb-Parsy, A. Moffett, L. Moore, O. A. Bayraktar, S. A. Teichmann, M. Y. Turco, R. Vento-Tormo, Mapping the temporal and spatial dynamics of the human endometrium in vivo and in vitro. *Nat. Genet.* **53**, 1698–1711 (2021).
155. Z. Cang, Y. Zhao, A. A. Almet, A. Stabell, R. Ramos, M. V. Plikus, S. X. Atwood, Q. Nie, Screening cell–cell communication in spatial transcriptomics via collective optimal transport. *Nat. Methods* **20**, 218–228 (2023).
156. T. Abdelaal, S. Mourragui, A. Mahfouz, M. J. T. Reinders, SpaGE: Spatial gene enhancement using scRNA-seq. *Nucleic Acids Res.* **48**, –e107 (2020).
157. M. S. Keller, I. Gold, C. McCallum, T. Manz, P. V. Kharchenko, N. Gehlenborg, Vitessce: Integrative visualization of multimodal and spatially resolved single-cell data. *Nat. Methods* **22**, 63–67 (2025).
158. D. Schapiro, H. W. Jackson, S. Raghuraman, J. R. Fischer, V. R. T. Zanotelli, D. Schulz, C. Giesen, R. Catena, Z. Varga, B. Bodenmiller, histoCAT: Analysis of cell phenotypes and interactions in multiplex image cytometry data. *Nat. Methods* **14**, 873–876 (2017).
159. N. Eling, N. Damond, T. Hoch, B. Bodenmiller, *cytomapper*: An R/Bioconductor package for visualization of highly multiplexed imaging data. *Bioinformatics* **36**, 5706–5708 (2021).
160. G. Palla, H. Spitzer, M. Klein, D. Fischer, A. C. Schaar, L. B. Kuemmerle, S. Rybakov, I. L. Ibarra, O. Holmberg, I. Virshup, M. Lotfollahi, S. Richter, F. J. Theis, Squidpy: A scalable framework for spatial omics analysis. *Nat. Methods* **19**, 171–178 (2022).
161. C.-H. L. Eng, M. Lawson, Q. Zhu, R. Dries, N. Koulena, Y. Takei, J. Yun, C. Cronin, C. Karp, G.-C. Yuan, L. Cai, Transcriptome-scale super-resolved imaging in tissues by RNA seqFISH+. *Nature* **568**, 235–239 (2019).
162. R. R. Stickels, E. Murray, P. Kumar, J. Li, J. L. Marshall, D. J. Di Bella, P. Arlotta, E. Z. Macosko, F. Chen, Highly sensitive spatial transcriptomics at near-cellular resolution with Slide-seqV2. *Nat. Biotechnol.* **39**, 313–319 (2021).
163. C.-S. Cho, J. Xi, Y. Si, S.-R. Park, J.-E. Hsu, M. Kim, G. Jun, H. M. Kang, J. H. Lee, Microscopic examination of spatial transcriptome using Seq-Scope. *Cell* **184**, 3559–3572.e22 (2021).
164. Y. Liu, M. Yang, Y. Deng, G. Su, A. Enninful, C. C. Guo, T. Tebaldi, D. Zhang, D. Kim, Z. Bai, E. Norris, A. Pan, J. Li, Y. Xiao, S. Halene, R. Fan, High-spatial-resolution multi-omics sequencing via deterministic barcoding in tissue. *Cell* **183**, 1665–1681.e18 (2020).
165. Y. Lee, D. Bogdanoff, Y. Wang, G. C. Hartoularos, J. M. Woo, C. T. Mowery, H. M. Nisonoff, D. S. Lee, Y. Sun, J. Lee, S. Mehdizadeh, J. Cantlon, E. Shifrut, D. N. Ngyuen, T. L. Roth, Y. S. Song, A. Marson, E. D. Chow, C. J. Ye, XYZeq: Spatially resolved single-cell RNA sequencing reveals expression heterogeneity in the tumor microenvironment. *Sci. Adv.* **7**, eabg4755 (2021).
166. S. R. Srivatsan, M. C. Regier, E. Barkan, J. M. Franks, J. S. Packer, P. Grosjean, M. Duran, S. Saxton, J. J. Ladd, M. Spielmann, C. Lois, P. D. Lampe, J. Shendure, K. R. Stevens, C. Trapnell, Embryo-scale, single-cell spatial transcriptomics. *Science* **373**, 111–117 (2021).

Acknowledgments: We thank K.P. Matchett, J.R. Portman, I.W.J. Fox, and J.R. Wilson-Kanamori for helpful discussions. **Funding:** This work was supported by a Wellcome PhD Clinical Training Fellowship (to P.P.V.), a Wellcome Senior Research Fellowship in Clinical Science (ref. 219542/Z/19/Z), Chan Zuckerberg Initiative Seed Network Grant, and a United European Gastroenterology Research Prize (to N.C.H.). **Competing interests:** N.C.H. has received research funding from AbbVie, Pfizer, Gilead, and Boehringer-Ingelheim and is an advisor or consultant for AstraZeneca, AbbVie, GSK, and MSD. P.P.V. and R.E.A. declare that they have no competing interests.

Submitted 31 July 2024
Accepted 19 March 2025
Published 9 April 2025
10.1126/scitranslmed.adm6783

Downloaded from https://www.science.org at Shanghai Jiao Tong University on June 30, 2025